



Cite this: *J. Mater. Chem. B*,
2024, 12, 5769

Recent advances in stimuli-responsive controlled release systems for neuromodulation

Jielin Shi,^{†,a} Chao Tan,^{†,a} Xiaoqian Ge,^b Zhenpeng Qin^{id, *bcde} and
Hejian Xiong^{id, *af}

Neuromodulation aims to modulate the signaling activity of neurons or neural networks by the precise delivery of electrical stimuli or chemical agents and is crucial for understanding brain function and treating brain disorders. Conventional approaches, such as direct physical stimulation through electrical or acoustic methods, confront challenges stemming from their invasive nature, dependency on wired power sources, and unstable therapeutic outcomes. The emergence of stimulus-responsive delivery systems harbors the potential to revolutionize neuromodulation strategies through the precise and controlled release of neurochemicals in a specific brain region. This review comprehensively examines the biological barriers controlled release systems may encounter *in vivo* and the recent advances and applications of these systems in neuromodulation. We elucidate the intricate interplay between the molecular structure of delivery systems and response mechanisms to furnish insights for material selection and design. Additionally, the review contemplates the prospects and challenges associated with these systems in neuromodulation. The overarching objective is to propel the application of neuromodulation technology in analyzing brain functions, treating brain disorders, and providing insightful perspectives for exploiting new systems for biomedical applications.

Received 4th April 2024,
Accepted 20th May 2024

DOI: 10.1039/d4tb00720d

rsc.li/materials-b

1. Introduction

Neuromodulation is the physiological process of regulating neural activity through the targeted delivery of stimuli, such as electrical stimulation or chemical agents, to specific neural structures within the body. Various neurochemicals, including neurotransmitters (e.g., acetylcholine, dopamine, glutamate, and GABA) and neuromodulators (e.g., ions, amino acids, and peptides) modulate neural physiological and pathological

processes in the central nervous systems. Chemical neuromodulation relies on the delivery of neurochemicals to the targeted brain regions, which bind to specific receptors or channels on the cell membrane to activate or inhibit neural activities.^{1,2} Chemical neuromodulation provides a powerful tool to investigate signal transmission and processes in the central nervous system.³ It is also useful for the treatment of movement disorders, pain, and depression in the clinic.^{4–6} Beyond endogenous membrane receptors, chemogenetic

^a Key Laboratory of Mental Health of the Ministry of Education, Guangdong-Hong Kong-Macao Greater Bay Area Center for Brain Science and Brain-Inspired Intelligence, Guangdong-Hong Kong Joint Laboratory for Psychiatric Disorders, Guangdong Province Key Laboratory of Psychiatric Disorders, Guangdong Basic Research Center of Excellence for Integrated Traditional and Western Medicine for Qingzhi Diseases, Department of Neurobiology, School of Basic Medical Sciences, Southern Medical University, Guangzhou, China. E-mail: hjxiong@smu.edu.cn

^b Department of Mechanical Engineering, The University of Texas at Dallas, Richardson, TX 75080, USA

^c Department of Biomedical Engineering, University of Texas Southwestern Medical Center, Dallas, TX 75390, USA

^d Department of Bioengineering, The University of Texas at Dallas, Richardson, TX 75080, USA

^e Center for Advanced Pain Studies, The University of Texas at Dallas, Richardson, TX 75080, USA. E-mail: Zhenpeng.Qin@utdallas.edu

^f Department of Cardiovascular Surgery, Zhujiang Hospital, Southern Medical University, Guangzhou, China

† These authors contributed equally to this work.



Hejian Xiong

Dr Hejian Xiong is a professor at Southern Medical University. He obtained his BS degree from Hubei University in 2012 and PhD degree in polymer chemistry from Changchun Institute of Applied Chemistry, Chinese Academy of Sciences in 2018. He worked as a postdoctoral with Prof. Zhenpeng Qin at the University of Texas at Dallas from 2018 to 2023. His current research focuses on developing functional nanoparticles for brain disease treatment and neuromodulation.

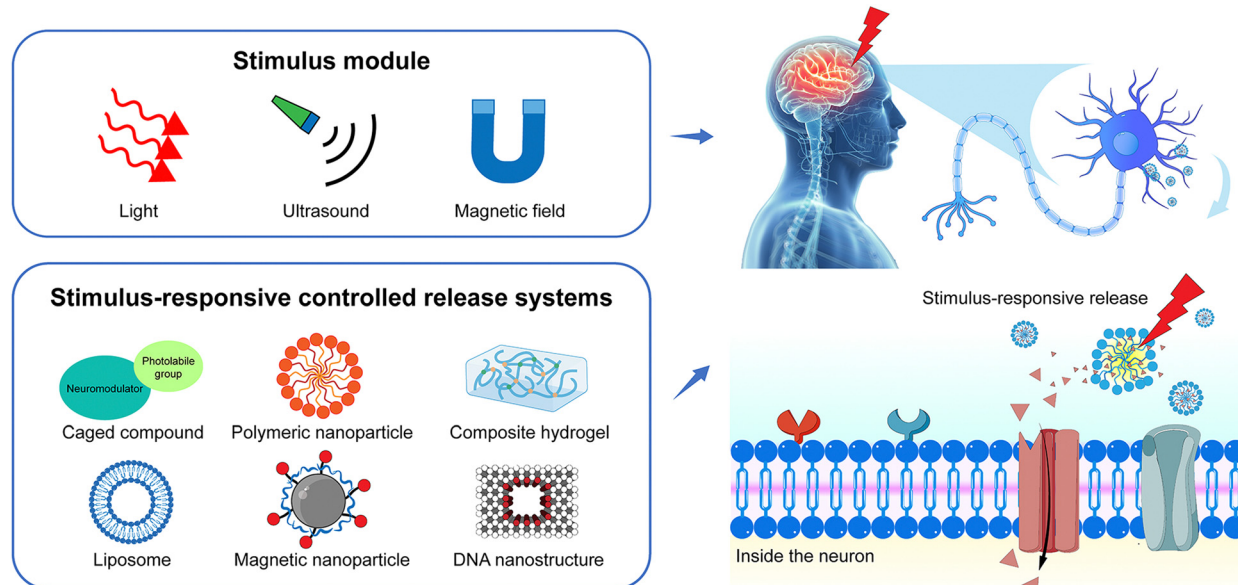


Fig. 1 Overview of stimulus-responsive controlled release system for neuromodulation. The delivery system releases neuroactive substances accurately in response to endogenous or exogenous stimuli, with the aim of activating, inhibiting and/or regulating receptors or ion channels on the neuron cell membrane.

strategies, such as the employment of the designer receptors exclusively activated by designer drugs (DREADDs), have been developed to improve the spatial and temporal modulation of G protein signaling *in vivo*.⁷ Due to the promising translational applications, chemical neuromodulation through various neuromodulators gains increasing interest.^{8,9} In the development of neuromodulation modalities aimed at increased specificity and reduced invasiveness, it is necessary to precisely control the distribution of neurochemicals within the brain, ensuring high spatiotemporal resolution for precise chemical neuromodulation.¹⁰

Recently, the development of stimuli-responsive controlled release systems offers new opportunities for precise chemical neuromodulation.¹¹ Neuromodulators can be loaded into the delivery systems, such as liposomes or polymeric nanoparticles, and released at the targeted area under optical, acoustic, or magnetic stimulation (Fig. 1). The stimuli-responsive delivery systems take advantage of the traditional methods of drug administration, such as increasing the stability of neuromodulators especially neuropeptides *in vivo*, and enhancing the accumulation in the brain.^{12,13} More importantly, the controlled release of neuromodulators in the local brain can facilitate the study of fast signal transmission in the brain. For example, Xiong *et al.* measured the spatiotemporal scale of neuropeptide volume transmission in the mouse cortex by the rapid neuropeptide release from gold-coated liposomes under the irradiation of near-infrared (NIR) laser pulses and optical sensing.¹⁴ On the other hand, stimuli-responsive delivery systems can enhance the efficacy of neuromodulation and reduce the side effects of neuromodulators. For example, Lea-Banks *et al.* demonstrated that localized anesthesia could be achieved by focus ultrasound-induced release from pentobarbital-loaded nanodroplets with lipid shell and decafluorobutane core in a

specific brain region without disrupting the blood–brain barrier (BBB) and off-target effects.¹⁵

Stimuli-responsive materials have garnered significant attention due to their potential applications in targeted drug delivery, tissue engineering, biosensing, and theranostics. As mentioned above, the emerging stimuli-responsive controlled release systems also offer powerful tools for precise neuromodulation. Herein, we summarize the recent advances in fabricating stimuli-responsive materials for neuromodulation for the first time and provide insights into developing the next generation of stimuli-responsive materials for safe, effective, and precise neuromodulation. We focus on two key aspects: the biological barrier for neuromodulator delivery and the innovations in the delivery systems for neuromodulation. We first discuss how the BBB extracellular space and matrix work as the biological barrier for targeted neuromodulator delivery. Next, we summarize the recent development of stimuli-responsive controlled systems for neuromodulation from the perspective of different external triggers, including light, ultrasound, and magnetic fields. We emphasize the design of controlled release systems and the release mechanism. Finally, we provide an outlook on future endeavors toward more safe and precise chemical neuromodulation techniques.

2. Biological barrier for delivery of neuromodulators to the brain

To achieve the desired outcomes of neuromodulators in the brain, controlled release systems must be accurately delivered to specific brain regions. Currently, delivery methods include intravenous injection and intracerebral injection into targeted areas. The systemic route offers convenience and non-invasiveness compared with the intraparenchymal injection,

but its effectiveness is considerably reduced by the BBB.^{16–18} The BBB, a selectively permeable barrier comprised of brain microvascular endothelial cells linked by tight junctions and surrounded by pericytes and astrocytic endfeet, maintains brain homeostasis by regulating molecular transport and protecting the brain from blood-borne toxins and pathogens. However, it also blocks over 98% of small-molecule drugs and all macromolecular therapeutics from entering the brain.^{19–21} To bypass the BBB, delivery systems can be modified with a targeting ligand (e.g., a monoclonal antibody or peptide) that binds to specific receptors, facilitating transcellular transport.^{22–25} This method of active targeting is advancing rapidly for treating brain diseases, including tumors, Alzheimer's disease, and Parkinson's disease, and could potentially be utilized for neuromodulator delivery.²⁰ Furthermore, using focused ultrasound in conjunction with microbubbles to temporarily enhance BBB permeability represents a novel physical approach, improving the delivery efficiency of therapeutics.^{26,27} In a similar vein, nanodroplets containing decafluorobutane and an anesthetic drug, activated by focused ultrasound, have successfully breached the BBB to administer the drug directly to targeted regions, achieving localized anesthesia in the motor cortex of rat.^{15,28} Recently, Qin *et al.* introduced an innovative technique for optically modulating the BBB through laser stimulation of gold nanoparticles targeted at tight junctions, enhancing the permeability of both the BBB and the blood-spinal cord barrier.^{21,29} Employing this technique enabled the administration of bombesin to the spinal cord, effectively inducing itch responses in mice.

Irrespective of the method used for administering delivery systems to the brain, all such systems and the neuromodulators they release must traverse a considerable distance within the narrow extracellular space (ECS) to reach their target neurons and elicit effects. The ECS's heterogeneity in width, with an average estimated at 40–60 nm based on quantum dots diffusion analysis,³⁰ poses a significant challenge to nanoparticle diffusion. In addition to ECS geometry, the extracellular matrix—comprising proteoglycans, hyaluronan, and various

small linking proteins—serves as an additional barrier to drug distribution within the brain (Fig. 2). For instance, the presence of increasing malignancy in astrocytic tumors has been shown to slow ECS diffusion due to glycoprotein production.³¹ Moreover, treatment with hyaluronidase has been shown to accelerate neuropeptide transmission in the mouse cortex.³² Nance *et al.* demonstrated that enhancing the surface density of poly(ethylene glycol) (PEG) on 40 nm and 100 nm polymeric nanoparticles can facilitate diffusion in human and rat brain ECS.³³ It is noteworthy that neuromodulators typically require binding to specific receptors on the cell membrane, resulting in minimal brain cell uptake. Song *et al.* reported that PEGylation of poly(lactic acid) surfaces reduces internalization by neurons, astrocytes, and microglia, whereas aldehyde modification has the opposite effect.³⁴ Furthermore, the surface charge of nanoparticles critically influences their brain ECS distribution. Dante *et al.* showed that negatively charged inorganic nanoparticles tend to interact with neuronal membranes and accumulate at the synaptic cleft, in contrast to positively and neutrally charged nanoparticles, which showed no neuronal association.³⁵ The success of neuromodulation significantly depends on the fate of delivery systems within the brain ECS, warranting further research.

3. Stimuli-responsive controlled release systems for neuromodulation

Stimuli-responsive controlled-release systems can deliver neurochemicals to targeted neurons when triggered by physical or chemical stimuli. Such systems are typically composed of nano-carriers with stimuli-responsive units and neurochemicals aimed at particular receptors or channels (Table 1). Most neurochemicals are hydrophilic, which can be conjugated to the nano-carriers with a stimuli-responsive linker or physically encapsulated in the hydrophilic space of nano-carriers. The stimuli-responsive unit is primarily designed to respond to

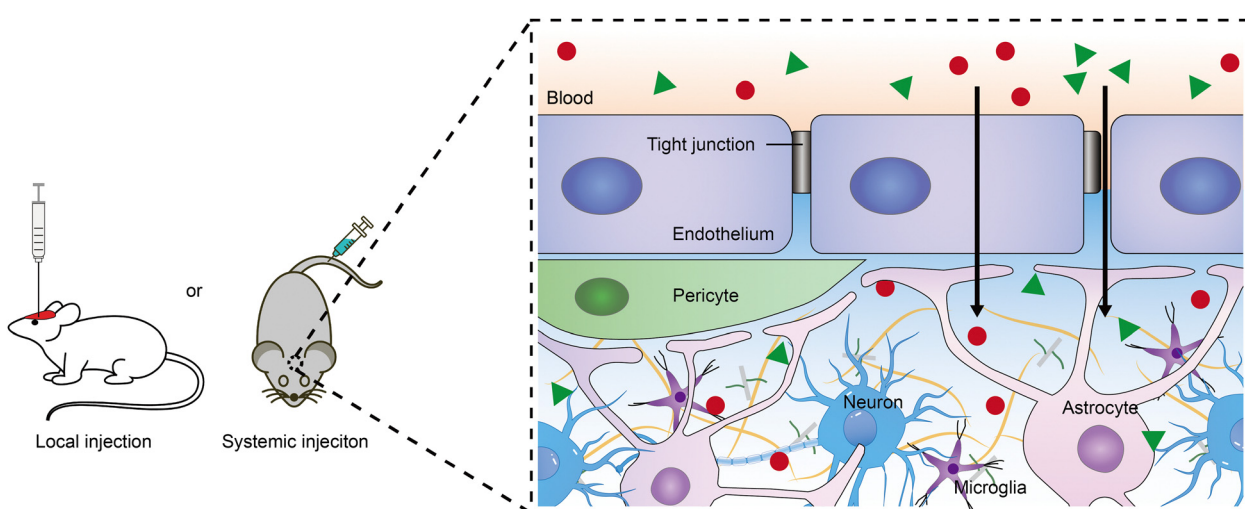


Fig. 2 Biological barrier for delivery of neuromodulators to the brain.

Table 1 Summary of recent advances in the stimulus-responsive controlled release systems for neuromodulation

Stimulus-responsive module	Release mechanism	Delivery systems	Cargo	<i>In vitro</i> effect	<i>In vivo</i> effect	Advantages	Ref.
Light-responsive	Photolysis	Caged compound	Opioid neuropeptides	Activating mu opioid receptor-coupled K ⁺ channels	—	Rapid release	36
	Photolysis	Caged compound	Neuropeptides: gastrin-releasing peptide, oxytocin, substance P, cholecystokinin	—	Neuropeptide signaling in intact tissue preparations	Precise spatial and temporal control of neuropeptide signaling	37
	Photolysis	Caged compound	Mu opioid receptor-selective peptide agonist	—	Rapid, opioid-dependent increase in mouse ventral tegmental area	Rapid behavioral changes observable, high spatio-temporal precision	38
	Photolysis	Caged compound	Opioid receptor agonists	—	Activation of various brain regions induced local alterations in receptor occupancy, metabolic activity, and affected pain and reward-related behaviors	High spatio-temporal precision in drug delivery and receptor activation	39
	Photolysis	DNA nanostructure	Glutamic acid loads cargo with photolabile linker	Activating Ca ²⁺ signaling pathways in primary hippocampal neurons	—	Controlled release of a wide range of bioactive molecules	40
	Photolysis	DNA nanostructure loaded with photo-responsive polymers	DHEA	Revealing the kinetics of neuronal activation	Spatial control at the level of single endosomes within a single cell	Triggered release with spatial and temporal precision at designated cells	41
	Photolysis	Upconversion nanoparticle coated by zeolitic imidazolate framework-8	Nitrosothiol	Activating the differentiation pathway for a markedly pronounced outgrowth of neuronal processes	Fostering the regrowth of damaged motor neuron axons in zebrafish and enhanced motor function recovery in rats following traumatic spinal cord injury	The pleiotropic effects of NO	42
	Photoisomerization	Photoswitchable nanovesicle	SKF81297	Activating cultures of primary striatal neurons	—	Highly controllable molecular release	43
	Photothermal	Liposomes containing a photosensitizer and gold nanorods	Tetrodotoxin or other nerve-blocking agents	—	Local anesthetic	—	44–46
	Photothermal	Polymeric nanoparticle with photosensitive PDPP	Fasudil	—	Significantly reducing the firing frequency of ventral tegmental area dopamine neurons involved in depression-like behaviors	—	47
Photomechanical	Photothermal	pNIPAM composite hydrogel embedded with PPy nanoparticles	Netrin or semaphorin 3A; glutamate	Triggering local signal transduction in a neural network or neuronal cell sub-domain with micro-scale precision	Remote control of brain activity	Versatility and ease-of-use	48
	Photomechanical	Liposomes tethered hollow gold nanoshells	Glutamate, potassium chloride, muscimol, and specific dopamine agonists	—	Repeated and stable neural manipulation modulated by laser intensity	Controlled release of a wide range of chemicals	49
	Photomechanical	Liposomes with gold nanoparticles coating	IP3	Triggering calcium signaling in cancer cells and primary DRG neurons through the release of IP3	—	Rapid release	50
	Photomechanical	Rad-PC-Rad nanovesicles coated with gold	IP3	Rapid unpacking of IP3 triggers intracellular Ca ²⁺ dependent	Enabling biomolecules to be released up to 4 millimeters in the rodent brain	High photosensitivity	51

Table 1 (continued)

Stimulus-responsive module	Release mechanism	Delivery systems	Cargo	In vitro effect	In vivo effect	Advantages	Ref.
	Photodynamic	Liposomes with NIR-absorbing photosensitizer	Tetrodotoxin	— signaling pathways in living cells	Sciatic nerve blockade	—	52 and 53
Ultrasound- responsive	Sono-mechanical	Liposomes tethered to microbubbles	Muscimol	—	Focal modulation of the propagation of neuronal activity in the rodent vibrissae sensory-motor pathway	High target specificity	54
	Sono-mechanical	Nanoemulsions with a block copolymer matrix and a liquid per-fluorocarbon (PFP) core	Propofol	—	Silencing of seizure activity <i>in vivo</i>	Noninvasive targeted transcranial neuromodulation	55
	Sono-mechanical	Nanoemulsions with a PEG-PLGA block copolymer matrix and a liquid PFP core	Propofol	—	Noninvasive mapping of the changes in functional network connectivity associated with pharmacologic action at a particular brain target	—	56
	Sono-mechanical	Nanodroplets with liquid deca-fluorobutane core	Pentobarbital and a GABA _A receptor agonist	—	Inducing local anesthesia in the motor cortex of rats	—	15 and 28
	Sonodynamic	Liposome with unsaturated lipids and protoporphyrin IX	Tetrodotoxin	—	Sciatic nerve blockade	On-demand local anesthesia	57 and 58
Magnetic field- responsive	Magnetic-thermal	Iron oxide MNPs and thermally labile linkers	Allyl isothiocyanate	Triggering Ca ²⁺ influx and action potential firing	—	Low required concentration	59
	Magnetic-thermal	Polymeric nanoparticles based on MNPs and poly(sebacic acid) composites	Protons	Remote triggering acid-sensing ion channels to evoke intracellular calcium influx in neurons	—	Wireless modulation of local pH	60
	Magnetic-thermal	Thermally responsive liposomes loaded with MNPs	CNO, SKF-38393 SCH-23390	— Providing precise molecular control over neural circuits and enabling rapid activation of both genetically engineered and naturally expressed receptors	— Interrogating pharmacologically targeted neural populations in subjects that are freely moving	61	
	Magnetic-thermal	Polymeric nanoparticles with MNPs and poly(oligo (ethylene glycol) methyl ether methacrylate) brushes	Dopamine	Enhancing the activity of ~50% of striatal neurons subjected to the treatment	— On-demand release of multiple microdoses	62	
	Magneto-mechanical	MNPs in Ca ²⁺ cross-linked hydrogels	Levodopa	Stimulating the proliferation of dopaminergic neurons and the expression of dopaminergic phenotype	—	63	

endogenous (e.g., pH, redox) or exogenous (e.g., light, sound, magnetic fields) stimuli.

Only a few studies have reported the endogenous stimulus-responsive systems for neuromodulation. Lei *et al.* activated or blocked the neuromicroenvironment in pancreatic cancer by loading Ferritin nanoparticles with the muscarinic agonist carbachol and the muscarinic antagonist atropine, respectively.

The Ferritin nanoparticles can release drugs in the weakly acidic environment (pH 6.5) of pancreatic tumors, and the drugs are further released in the lysosomes (pH 5.0) of tumor cells to modulate the early invasive growth and metastatic spread of pancreatic cancer progression.⁶⁴ Zuo *et al.* crafted an amphiphilic block copolymer incorporating boron-based reactive oxygen species (ROS) scavengers to deliver the KCC2

agonist CLP-257 to the targeted areas affected by spinal cord injury.⁶⁵ This nano-carrier exhibits high sensitivity to ROS stimulation, mitigates the accumulation of ROS in the lesion area, and activates the dormant neural circuits by stimulating the KCC2 gene and reducing the excitability of inhibitory interneurons. In addition, gasotransmitters such as nitric oxide (NO), hydrogen sulfide, and carbon monoxide can be released from the corresponding donors in the presence of enzymes or intercellular reducing agents such as glutathione and play crucial roles in synaptic plasticity and neural communication.^{66–68} Modifying the gasotransmitter donor with peptides or targeted substances to form nanoparticles can improve the stability and efficacy of gasotransmitters. For example, Pal *et al.* developed a new method for delivering NO by combining a self-assembling peptide with a nitrated aspirin to form soft nanospheres that can control and sustain the release of NO in the presence of intercellular glutathione. The platform displayed a significantly greater amount of NO release in cellular environments, leading to neurite outgrowth.⁶⁹

In terms of external stimuli, optical stimulation stands out for its high spatial and temporal resolution but with limited penetration depth ($\sim 1\text{--}1.5$ mm).⁷⁰ Acoustic stimulation, especially through non-invasive methods like focus ultrasound (FUS), possesses the capacity to penetrate deep tissues (>50 mm) with a spatial resolution inversely related to the penetration depth (in general >1 mm³ and temporal precision >10 ms).^{71,72} Furthermore, magnetic fields are recognized for their non-invasiveness and ability to access deep brain regions with little attenuation, presenting clinical pathways for treating neurological and psychiatric disorders.⁷³ The strategies to fabricate the controlled-release systems in response to these external stimuli are pretty similar to those used in drug delivery. For example, *o*-nitrobenzyl derivatives are commonly used for photolysis under a light stimulus to release the active neurochemical and gold nanoparticles are often used for photothermal triggered release. Meanwhile, micro/nano-bubbles are the most investigated delivery systems upon ultrasound stimulus and iron oxide nanoparticles are widely used for magnetic-thermal triggered release.

Despite the above similarity, delivering neurochemicals to the brain is challenging because of the complicated brain microenvironment and low active concentration of neurochemicals. Many advances have been made to develop various stimuli-responsive systems for neuromodulation, which are summarized below. Here, we delve into the unique attributes of each system and discuss the potential challenges and considerations pivotal to their application in neuromodulation.

3.1. Light-responsive

Expanding the spectral absorption range of materials into the NIR region has notably advanced the development of stimulus-responsive materials. The NIR spectrum (700–1700 nm), especially the second NIR window (NIR-II, 1000–1700 nm), offers distinct advantages over the visible spectrum (400–700 nm), including deeper tissue penetration and reduced phototoxicity.^{74,75} Consequently, this opens promising avenues for conducting neuroimaging

and neuromodulation studies in deep brain regions.^{76,77} Neuromodulation *via* light-induced release of neuroactive substances involves five main mechanisms: photolysis, photoisomerization, photothermal, photomechanical, and photodynamic mechanisms.

3.1.1. Photolysis mechanism. Photolysis is a chemical process in which the molecules are broken down into smaller parts after photon absorption. By employing light to catalyze changes within molecules, the modulation of neuronal activity achieves exceptional spatial and temporal accuracy. Caged compounds are probes sensitive to light that package biomolecules in an inactive state with photoremoveable protecting groups, which have been applied in various biomolecules such as neurotransmitters, neuropeptides, receptor agonists or antagonists, and metal ions.^{78,79} Once initiated by light at specific wavelengths, the caged compounds can recover the activity with kinetic rates at the microsecond level.^{80,81}

Banghart *et al.* used a dimethoxynitrophenethyl (DMNPE) caging group, which contains a neutral methyl group, affording light-sensitive forms of the mu-opioid receptor agonist oxymorphone and the antagonist naloxone: photoactivatable oxymorphone (PhOX) and photoactivatable naloxone (PhNX) (Fig. 3(a) and (b)).³⁹ These molecules can be photoactivated in the brain with sub-second flashes of light through implanted optical fibers to drive rapid changes in neural circuit function (Fig. 3(c)). *In vivo* experiments showed that photoactivation of PhOX and PhNX in the brain leads to alterations in various pain- and reward-related behaviors (Fig. 3(d)–(f)). This approach facilitates detailed studies of opioid-sensitive circuits in animals and minimizes side effects due to drug action at other sites. More recently, the same group introduced a cutting-edge biomimetic caging strategy by extending the C-terminus of neuropeptides with photocleavable amino acids to emulate pro-neuropeptides.³⁷ Furthermore, the group synthesized CNV-Y-DAMGO, a novel caged version of the μ -opioid receptor-selective peptide agonist DAMGO.³⁸ The carboxy-nitroveratryl (CNV) group is appended to the N-terminal tyrosine phenol of DAMGO, which reduces the affinity of DAMGO for mu-opioid receptors. Photoactivation at the ventral tegmental area led to a fast increase of locomotor activity of mice after the flash in 1 second, reaching a transient steady state within 2 seconds. However, most of the protecting groups are sensitive to UV and violet wavelengths and have to be compatible with fiber photometry for *in vivo* applications. Meanwhile, the caged compounds, especially caged peptides, are not stable *in vivo* due to the degradation induced by the peptidase.^{82,83} Jiang *et al.* employed NIR light to initiate the release of NO from the upconversion nano-carrier, through specific cleavage of the S-NO bond in the photochemical donor by light-converted UV energy. *In vivo* studies demonstrated that this system fostered the regrowth of damaged motor neuron axons in zebrafish and enhanced motor function recovery in rats following traumatic spinal cord injury.⁴²

The development of DNA technology has led to the emergence of various DNA-based materials with unique shapes and sizes through the classical Watson–Crick base pairing-enabled self-assembly. These structures can selectively release drugs in

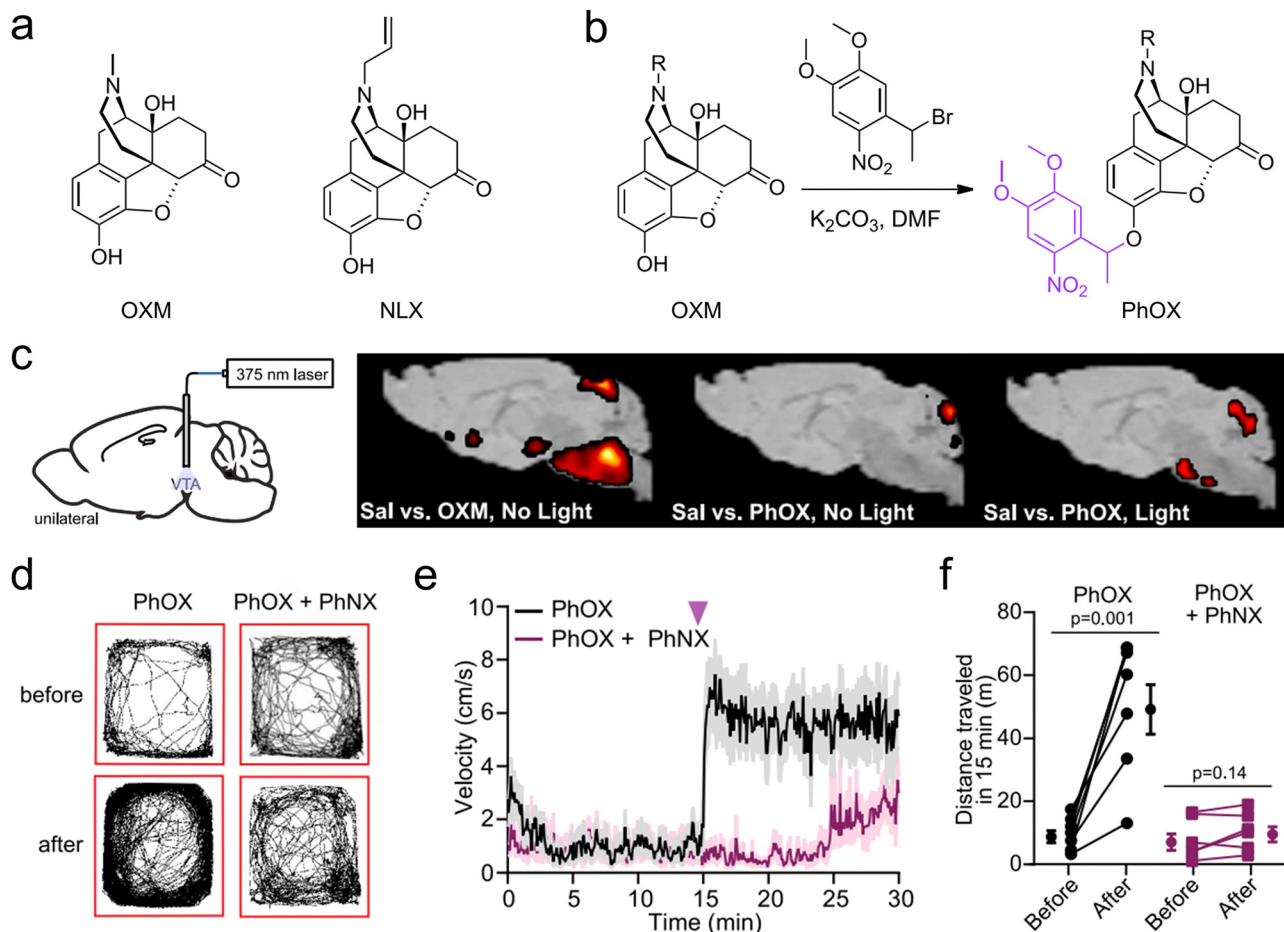


Fig. 3 (a) Chemical structures of OXM, NLX. (b) Reaction scheme depicting the one-step alkylation procedure used to synthesize PhOX and PhNX. (c) Schematic indicating the implantation of an optical fiber above the VTA and brain-wide voxel-based analysis of [¹⁸F]-FDG uptake. Color shaded areas represent clusters of voxels (R100) with significant increases in FDG accumulation compared with saline. (d)–(f) Example maps of open field locomotor activity, plot of average velocity over time and summary plot of the total distance traveled before or after photoactivation. Reproduced with permission.³⁹ Copyright 2023, Elsevier.

response to external stimuli by integrating different molecular switches.^{84,85} Kohman *et al.* utilized an innovative photosensitive cross-linker-labeled DNA origami to encapsulate molecules for 240–400 nm light-induced release (Fig. 4(a)).⁴⁰ This photolabile cross-linker features an *o*-nitrobenzyl (*o*-NB) motif for photocleavage, an azido group for coupling with alkyne-functionalized oligonucleotides, and an activated carbonate group for conjugation to cargo molecules possessing a free amino group. The cargoes encapsulated within the DNA nanocages range from small molecules to full-sized proteins. This approach demonstrated that glutamate-loaded DNA nanocage could trigger Ca²⁺ signaling in primary hippocampal neurons *in vitro* (Fig. 4(b) and (c)). Similarly, Veetil *et al.* used cell-targeted icosahedral DNA nanocapsules combined with light-responsive polymers to achieve light-induced targeted delivery of small molecules to specific cells of *C. elegans*.⁴¹ The DNA nanocapsules are constructed by icosahedral DNA assembly methods, with a large internal space capable of loading stimuli-responsive polymers. Dehydroepiandrosterone, a neurosteroid known for enhancing neurogenesis and neuronal survival, and

precisely controls when neurons are activated, is attached to 10 kDa dextran through a photocleavable 2,4-dimethoxy nitrobenzyl linker, and designed to be released upon photoirradiation at 400 nm. Modifications to the external surface of these nanocapsules enable targeting of specific cell types in *Caenorhabditis elegans*. Light-mediated release of DHEA immediately raised intracellular Ca²⁺ in neurons and revealed the kinetics of this precise neuronal activation. However, multifunctional polymer-DNA nanomaterials encounter several challenges, such as rapid metabolism, targeting inaccuracies, and instability, which currently restrict their clinical utility.⁸⁴

3.1.2. Photoisomerization mechanism. Photoisomerization hinges on the capacity of specific molecules to modify their conformation in response to light exposure. A prime instance of this phenomenon is the controlled isomerization of azobenzene under UV/visible light. Azobenzene is characterized by its thermodynamically stable *trans* form and a metastable *cis* form. Exposure to UV light induces a transition from the *trans* form to the *cis* form (*trans* → *cis*). Conversely, the *cis* structure can revert to the *trans* configuration (*cis* → *trans*)

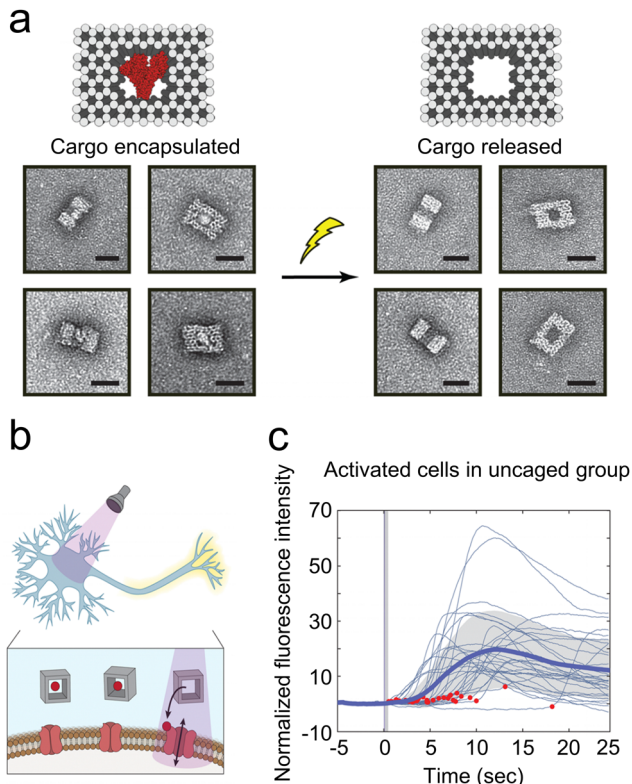


Fig. 4 (a) The activation of cargo release from nanocages upon light exposure. (b) A schematic representation illustrates the release of glutamate from a DNA nanocage triggered by UV light within the 240–400 nm range. This release activates neurons through the liberated glutamate. (c) The normalized fluorescence intensity, indicative of intracellular calcium levels, aligns with the initiation of illumination in cells from the uncaged group. A solid blue line denotes the average, with the standard deviation highlighted in gray. Red dots indicate moments of light exposure ($N = 30$ neurons). Reproduced with permission.⁴⁰ Copyright 2016, American Chemical Society.

when exposed to a particular wavelength of visible light or in darkness, thus realizing a fully reversible isomerization.^{86–88} Due to its photochromic attributes, azobenzene is a pivotal element in various molecular devices and functional materials. In recent years, two photon excitation of azobenzene photoswitches has been used in the field of neuromodulation, which can achieve precise manipulation of glutamate receptors (GluRs) on neuronal cell membranes.⁸⁹ Recent advancements have extended the application of photoswitches to lipids, named “Photolipids”, which contain an azobenzene group in their lipid tails. Photolipids are innovative tools for modulating lipid bilayer properties with light, including the photoswitchable phosphatidylcholine derivative, azo-PC. Upon illumination, azo-PC changes structural conformation, thus modifying its lateral interaction within the lipid bilayer.^{90–94} This functionality enables nanocarriers to dynamically control the release of cargo on demand through alterations in membrane permeability, presenting a novel approach for *in situ* manipulation of phospholipid bilayer membranes.^{95,96}

In a recent study, Xiong *et al.* introduced a new type of photoswitching nanovesicles called “azosome,” made by

adding azo-PC to precisely control neuronal activity.⁴³ Azo-PC can change shape reversibly when exposed to 365 nm and 455 nm light, significantly altering the lipid bilayer’s thickness (Fig. 5(a) and (b)). This change is due to the random arrangement of *cis*-azobenzene groups in the bilayer and the reduced thickness, which increases the permeability of the *cis*-azo-PC bilayer. By using 365 nm and 455 nm light, substances can be quickly released from the azosome in less than three seconds. This study demonstrated that SKF-81297, a drug that activates dopamine D1-receptors, could be released from the azosome, activating primary striatal neuron cultures (Fig. 5(c)). The release from photoswitchable nanovesicles does not cause any side effects such as heat or ROS, providing a safe and precise tool for neuromodulation.

3.1.3. Photothermal mechanism. For photothermal triggered release, the materials absorb incident light and change light energy into heat, rapidly elevating the temperature. The localized heat can induce a phase transition in the temperature-sensitive delivery systems, such as the destabilization of liposome membranes or the liquefaction of hydrogel matrices, leading to the controlled release of the encapsulated neuromodulators.^{97,98} Li *et al.* synthesized a drug delivery system composed of conjugated polymer as a photosensitive group and fasudil as the drug cargo to achieve photothermal modulation of depression-related ion channels by releasing drugs with NIR light.⁴⁷ The photothermal conversion efficiency of NPs-F was 57.48% under 808 nm laser irradiation, ensuring the nanoparticles reached 40–42 °C for the drug release in 50 s. Conjugated polymer nanoparticles successfully cross the BBB by increasing the permeability of the BBB through local heat generation, and significantly reduces firing frequency of ventral tegmental area dopamine neurons which are involved in depression-like behaviors. In parallel, the Kohane lab has made significant contributions to the field of local analgesia.^{44–46} By attaching gold nanorods to thermosensitive liposomes, tetrodotoxin (TTX) or other nerve-blocking agents can be released under the NIR light (Fig. 6(a)). Gold nanorods were synthesized with pronounced absorbance at 730 nm, coinciding with the peak absorbance wavelength of the photosensitizer in liposomes. These liposomes offer remotely regulated, sustained local anesthesia and enable a specified release event or degree of nerve blockade at reduced irradiance, enhancing safety, or achieving deeper tissue penetration at the same irradiance level (Fig. 6(b) and (c)). Furthermore, the development of low-temperature-sensitive liposomes with gold nanorods enables more efficient light absorption, minimizes thermal toxicity risks, and reduces the irradiation time needed for drug release.⁴⁶ 1-Palmitoyl-2-hydroxy-*sn*-glycero-3-phosphocholine is the key component of the low-temperature-sensitive liposomes, which could form nanopores in the liposomes at mild hyperthermia and accelerate the escape of the payload.

Composite hydrogels, which swell when heated to release drugs, have also proven useful in neural regulation.⁹⁹ Li *et al.* crafted microscale thermosensitive composite hydrogels from poly(*N*-isopropylacrylamide) (pNIPAM) infused with polypyrrole (PPy) nanoparticles. The pNIPAM hydrogel offers a thermally responsive capability, while the PPy nanoparticles serve as

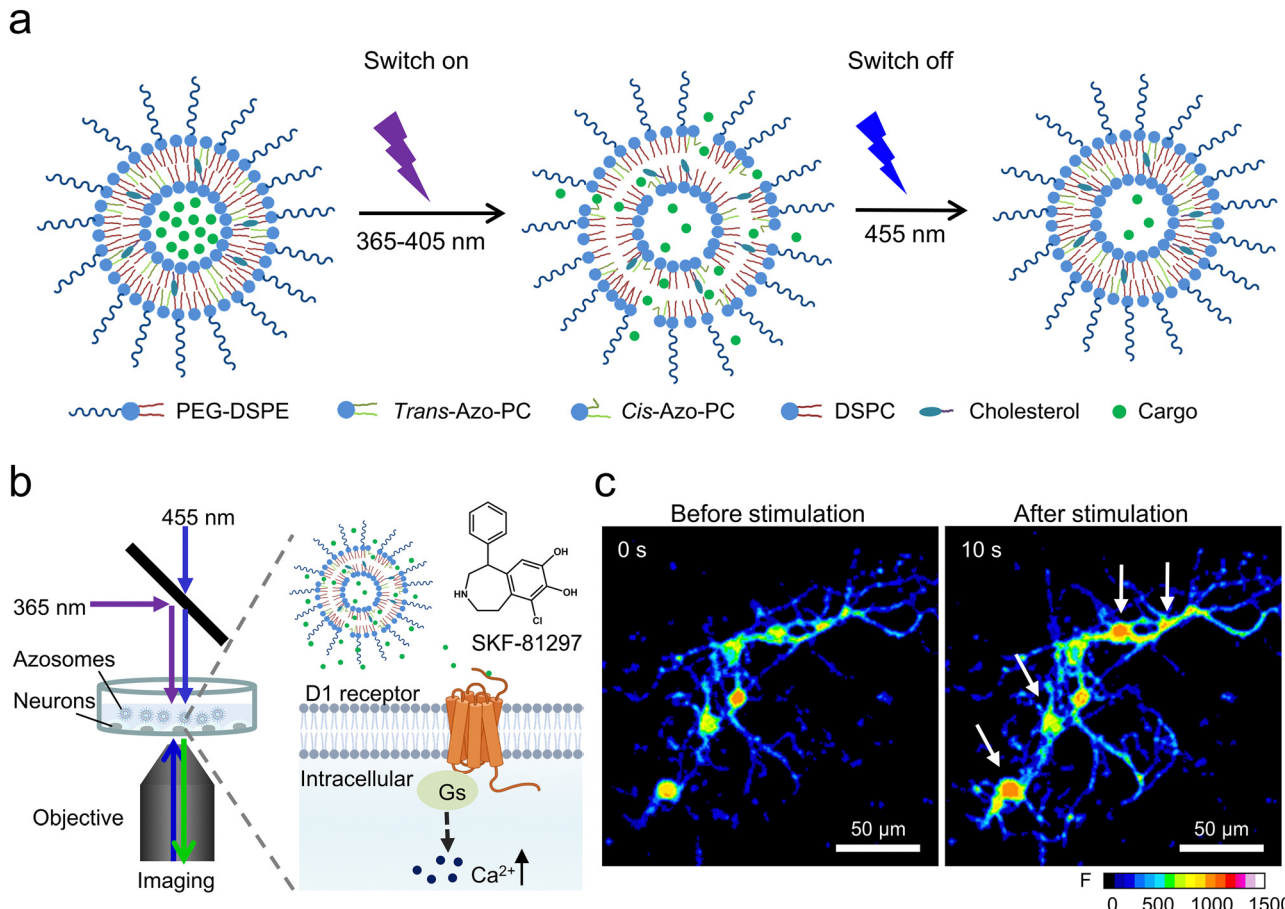


Fig. 5 (a) A diagram detailing the mechanism behind the release from azosomes that can be controlled by light. (b) An illustration showing how SKF-81297 is released from the azosome using light, leading to an influx of Ca^{2+} in primary mouse striatal neurons. (c) A real-time fluorescence visualization of primary mouse striatal neurons both prior to and following exposure to sequential 365 nm light (40 mW cm^{-2} , 0.5 s) and 455 nm light (40 mW cm^{-2} , 2 s). Fluo-4 serves as the calcium indicator. The scale bar represents 50 μm . Reproduced with permission.⁴³ Copyright 2023, Tsinghua University Press.

photothermal transducers. The system can deliver various neuro-modulating molecules, including small chemicals and large proteins, without relying on complex chemical bonding processes to link the molecules together.⁴⁸ NIR-triggered delivery of glutamate into the rat auditory cortex resulted in synchronized spiking activity, showcasing the potential for non-invasive neural modulation in living organisms. Similarly, other researchers have demonstrated thermoresponsive hydrogels of different designs can utilize the thermal effects generated by photoinduction for the targeted release of local anesthetics, thereby extending the drug's period of effectiveness.^{100,101} These investigations highlight the capability of photothermal methods to precisely modulate neural activity. Nonetheless, extensive research is necessary to thoroughly assess the long-term impacts and the safety of photothermal effects in living organisms.

3.1.4. Photomechanical mechanism. Nanomechanical transduction in plasma nanovesicles irradiated by a single, short laser pulse has shown great promise in neuromodulation. When subjected to ultrashort laser pulse irradiation (ps, fs), nanovesicles integrated with or coated by plasmonic gold structures rapidly heat to elevated temperatures. This heating stimulates the formation of transient nanoscale vaporizing

bubbles that undergo growth and rupture within nanoseconds, producing nanoscale mechanical effects that allow cargo to leak out of nanovesicles.^{102–104} For example, Nakano *et al.* linked hollow gold nanoshells (HGNs) to liposomes by thiol-gold interaction to develop a nano-carrier for the controlled release of neuromodulators (glutamate, potassium chloride, muscimol and specific dopamine agonists) upon exposure to an 890 nm femtosecond laser.⁴⁹ This system enables repeated, multiple releases and significantly impacts long-term synaptic plasticity (Fig. 7(a)). In a parallel study, Li *et al.* utilized NIR laser pulses to liberate cytoplasmic inositol triphosphate (IP3) from liposomes coated with gold nanoparticles ranging from 2.1 to 5.3 nanometers.⁵⁰ The phenomenon of strong plasmonic coupling among assemblies of gold nanoparticles induces a red shift in the localized surface plasmon resonance spectra. This shift not only augments the surface-enhanced Raman scattering properties but also significantly improves photothermal conversion efficiency.^{105–107} This technique facilitates cellular signaling activation in a non-thermal, ultrarapid, and exceptionally precise manner, underscoring the efficacy of photomechanical approaches in accurately governing intracellular processes without heat generation (Fig. 7(b)).

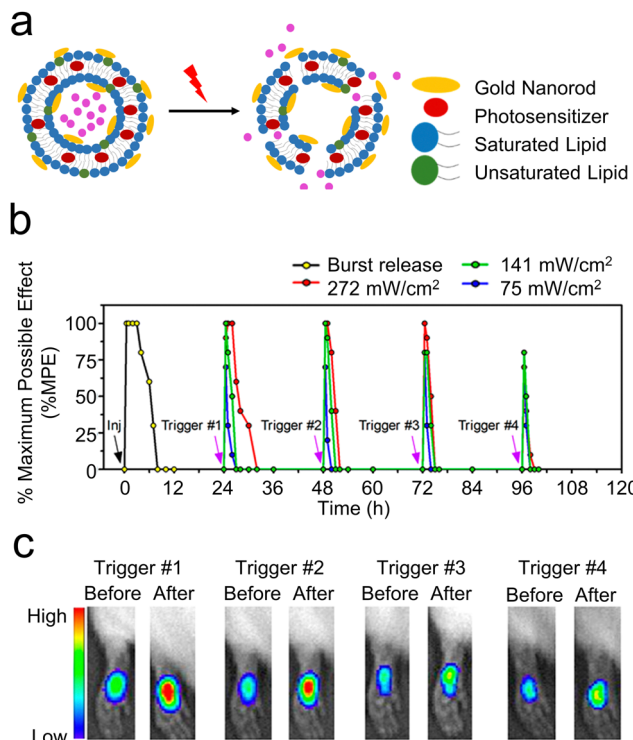


Fig. 6 (a) An illustrative diagram of liposomes designed for the light-induced release of medication. Reproduced with permission.⁴⁴ Copyright 2017, American Chemical Society. (b) An analysis of the local anesthetic impact on the footpad following the injection (indicated by a black arrow) of 100 μ L of liposomes and subsequent exposure to a NIR laser at 808 nm in a continuous wave at power densities of 75, 141, and 272 mW cm^{-2} for 10 minutes (highlighted by purple arrows). (c) The fluorescence of R6G observed using an *in vivo* imaging system both immediately before and after exposure to light at various times post-injection (24 h, 48 h, 72 h, and 96 h) into the rat footpad. Reproduced with permission.⁴⁵ Copyright 2016, American Chemical Society.

Furthermore, Xiong *et al.* constructed gold-coated mechanically responsive nanovesicles with the artificial phospholipid Rad-PC-Rad and gold-coating (Fig. 7(c)).⁵¹ They synthesized 1,3-diamidophospholipid Rad-PC-Rad by replacing the carboxylic acid ester part of the natural phospholipid with an amide bond. They also altered its structure at the glycerol backbone from the natural *sn*-1,2 to a *sn*-1,3 arrangement. With the particular structure, Rad-PC-Rad could form intermolecular H-bonding networks and d-shaped liposomes with defect edges, which are sensitive to shear stress.^{108,109} The gold coating on the surface of these nanovesicles can be activated by NIR picosecond laser pulses, thus creating nanomechanical stress and leading to almost complete vesicle cargo release in sub-seconds. This novel ultra-photosensitive nanovesicle system combined the mechano-responsive nanovesicles and light-induced nanomechanical force and achieved efficient release down to 4 mm deep in the mouse brain. Furthermore, there was no global heating from the gold-coated mechanically responsive nanovesicles under the NIR laser pulse irradiation, minimizing the side effects. This system provides a new avenue for remote neuromodulation in deep brain regions.

3.1.5. Photodynamic mechanism. In addition to the above methods, Kohane lab has engineered a photosensitive liposome with photosensitizer PdPC(OBu)8(18) for the photodynamically triggered release and on-demand nerve blockade.^{52,53} When exposed to NIR light, the photosensitizer PdPC(OBu) 8(18) generates ROS, leading to the peroxidation of unsaturated lipids within liposome membranes.⁸⁷ This chemical reaction initiates the formation of a new α -bond and a 1,5-hydrogen shift, transforming the lipid composition to a hydrophilic state. This alteration destabilizes the hydrophobic interactions essential for liposome integrity, thus facilitating the release of tetrodotoxin. Employing this innovative approach allows for multiple, adjustable instances of local anesthesia, demonstrating a significant advancement in controlled drug delivery mechanisms.¹¹⁰

3.2. Ultrasound-responsive

Contrary to invasive techniques such as deep brain stimulation and spinal cord stimulation, which require surgical implantation and pose complications, ultrasound represents a safer, non-invasive alternative for brain stimulation. Furthermore, FUS offers greater spatial precision (targeting region dimensions up to 1–2 mm^3) and the ability to effectively target deeper brain structures (several centimeters of penetration can be achieved clinically) than non-invasive methods such as transcranial electrostimulation and transcranial magnetic stimulation.⁷² Consequently, ultrasound neuromodulation has emerged as a potent instrument for investigating neural circuits and managing neurological disorders, attracting significant scientific interest. Sonogenetics, a novel neuromodulation approach derived from optogenetics and chemical genetics, employs acoustic stimulation to activate genetically modified expression of mechanosensory or temperature-sensitive ion channels, aiming to precisely modulate targeted neuronal populations.¹¹¹ In this study, we focus on the ultrasound-triggered release of neuromodulators rather than other ultrasound neuromodulation techniques.

3.2.1. Sono-mechanical mechanism. Ultrasonic waves can generate high-intensity localized pressure waves, including cavitation and radiation, that can lead to temperature increases, mechanical stress, and cell death. Sonoporation employs acoustic cavitation in the ultrasonic range to enhance the permeability of the cell plasma membrane, which is widely used in molecular biology and non-viral gene therapy to facilitate the uptake of large molecules into cells.¹¹² In recent years, interest in sonomechanical-mediated neuromodulation has gradually increased.¹¹³ Recent developments in nanoparticle technology and FUS devices have created promising opportunities for targeted drug delivery across the BBB. Airan *et al.* demonstrated that applying transcranial FUS to polyethylene glycol-polycaprolactone block copolymeric nanoemulsions with a liquid perfluorocarbon core could induce a phase transition of perfluorocarbon from liquid to gas (Fig. 8(a)).^{55,114} Propofol is a small molecule, fat-soluble drug that readily crosses the BBB and enters the brain through the bloodstream without compromising the integrity of the barrier. It is sonicated at a frequency of 1 MHz, allowing precise targeting within the brain (Fig. 8(b) and (c)). This approach significantly

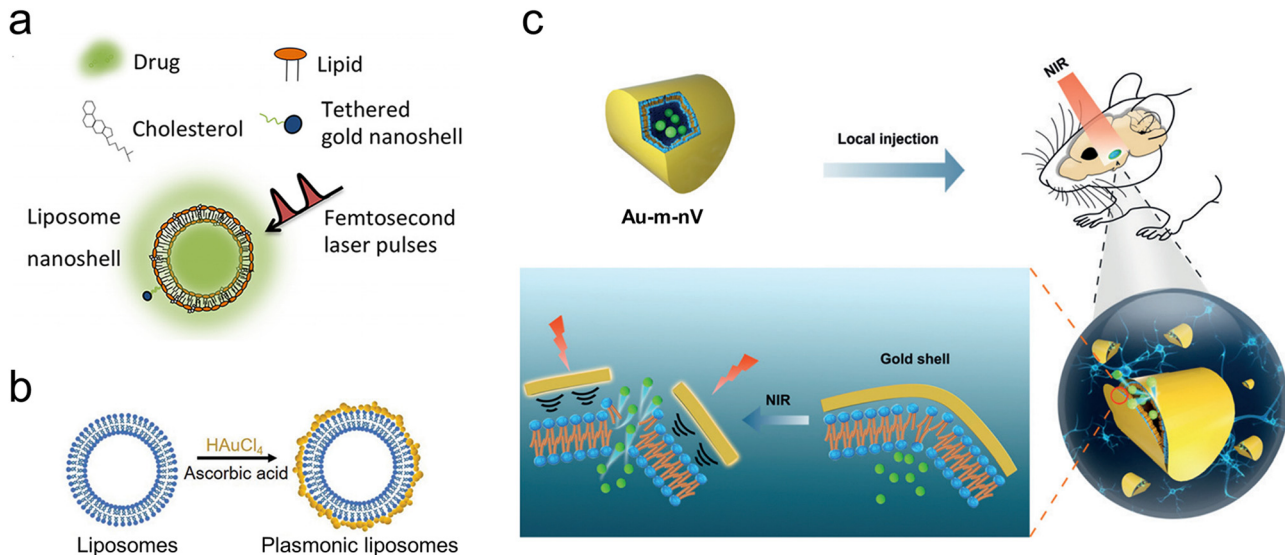


Fig. 7 (a) The assembly of liposomes incorporating gold nanoshells from their constituent parts. Reproduced with permission.⁴⁹ Copyright 2016, Society for Neuroscience. (b) The process of creating liposomes coated with plasmonic gold nanoparticles. Reproduced with permission.⁵⁰ Copyright 2017, Wiley-VCH. (c) Schematic illustration of NIR laser pulses triggered release using gold-coated nanovesicles (Au-m-nV) in deep brain regions. Reproduced with permission.⁵¹ Copyright 2020, Wiley-VCH.

mitigated seizures in an acute rat epilepsy model, demonstrating the potent neuromodulatory effects of propofol when released in

targeted brain regions. Moreover, the chemical properties of phase-change nanoparticles allow stable encapsulation of virtually

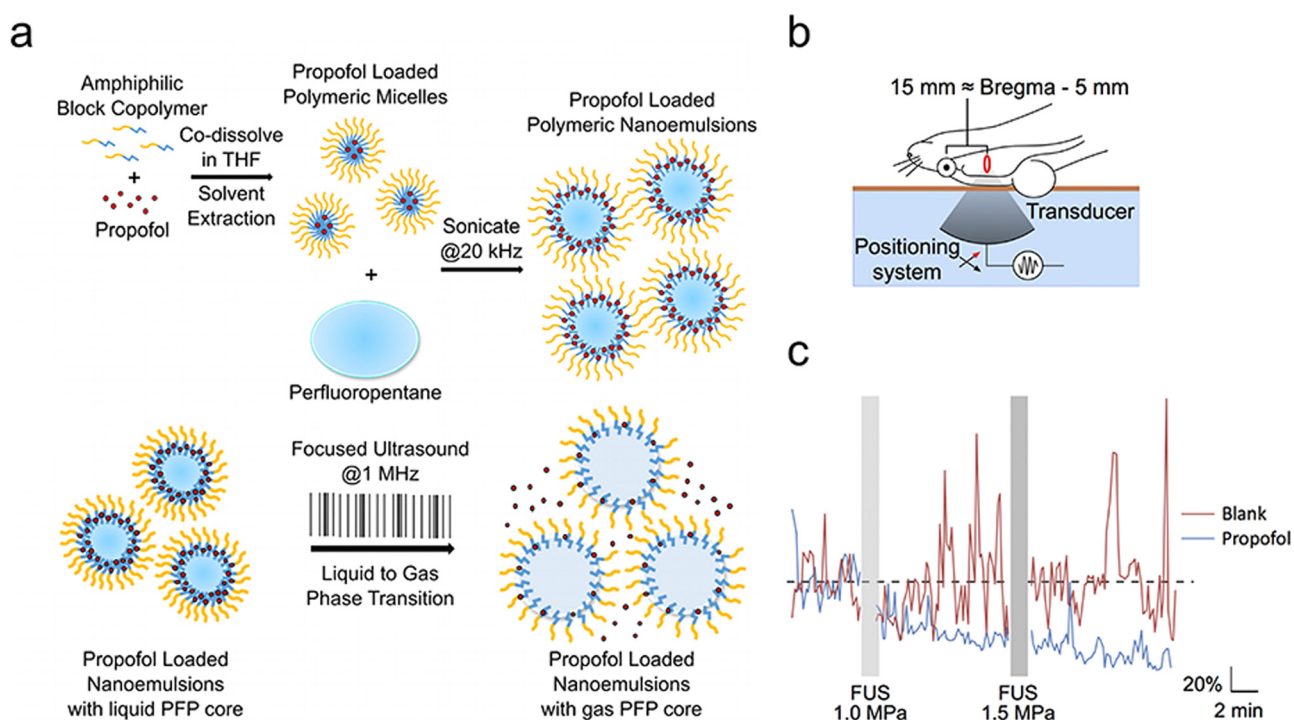


Fig. 8 (a) A diagram illustrating the preparation and application of nanoparticles designed for drug delivery, controlled by focused ultrasound. (b) The setup to test its effectiveness in live rats is shown. Rats had their back fur removed and were laid down on a bed designed for focused ultrasound. The setup used degassed water (light blue), a Kapton membrane filled with the same water (orange-brown), and ultrasound gel (not shown). Rats were then made to have seizures using the chemical pentylenetetrazole. (c) The overall EEG power, adjusted to a baseline and averaged across rats given nanoparticles with propofol (blue) versus those without any drug (blank, red), throughout the experiment (7 rats for propofol, 5 for blank). Grey bars indicate when the ultrasound (FUS) was used at specific high pressures, with 50 ms pulses every 1 second for 60 seconds. An electrical issue made it impossible to analyze EEG data during the ultrasound. Reproduced with permission.⁵⁵ Copyright 2017, American Chemical Society.

any hydrophobic small molecule drug. Given that hydrophobic small molecules can generally cross the BBB, phase-change nanoparticles could in principle, encapsulate almost any drug of neuropsychiatric interest. The same group further employed a similar design to demonstrate how ultrasonic drug uncaging induces changes in the network-level functional connectivity, showing that it causes secondary changes in brain regions connected to the sonicated target.⁵⁵ Similarly, Lea-Banks *et al.* utilized ultrasound-responsive nanodroplets to trigger the release of pentobarbital under FUS for the local anesthesia in the motor cortex of rats without compromising the BBB's integrity.²⁸ The same team also reported the spatial precision of this nanodroplet-mediated drug delivery within the brain through direct mapping of BBB-penetrating dye release in both a simulated tissue model and the rat brain.¹⁵ Noteworthy, ultrasound-responsive nanodroplets offer significant advantages as drug carriers with limited systemic spread, longer circulation times than traditional microbubbles, and a specific vaporization threshold for controlled drug release.¹¹⁵

Owing to the off-target effects within existing systemic treatments, central nervous system disorders pose significant

treatment challenges. Ozdas *et al.* implemented a groundbreaking method by systemically injecting engineered ultrasound-controllable drug carriers and then applying an innovative two component Aggregation and Uncaging Focused Ultrasound Sequence (AU-FUS) to targeted areas within the brain (Fig. 9(a)).⁵⁴ Ultrasound-controlled drug carriers were developed by attaching drug-filled liposomes to ultrasound-sensitive microbubbles. These microbubbles have a core made of perfluorocarbon gas, and the liposomes can enclose a broad spectrum of small-molecule drugs. The attachment process utilizes thiol-maleimide chemistry, creating a carrier responsive to ultrasound for precise drug delivery. The initial sequence congregates drug carriers with millimeter accuracy in large numbers. The subsequent sequence releases the carrier's contents locally, ensuring high specificity towards the target without breaching the BBB. After the release, the drug can pass through the intact BBB locally (Fig. 9(b) and (c)). This approach allows for the circuit-specific modulation of sensory signaling in the motor cortex of rats by concentrating and liberating a GABA_A receptor agonist from the ultrasound-controlled carriers. Notably, this method uses substantially less

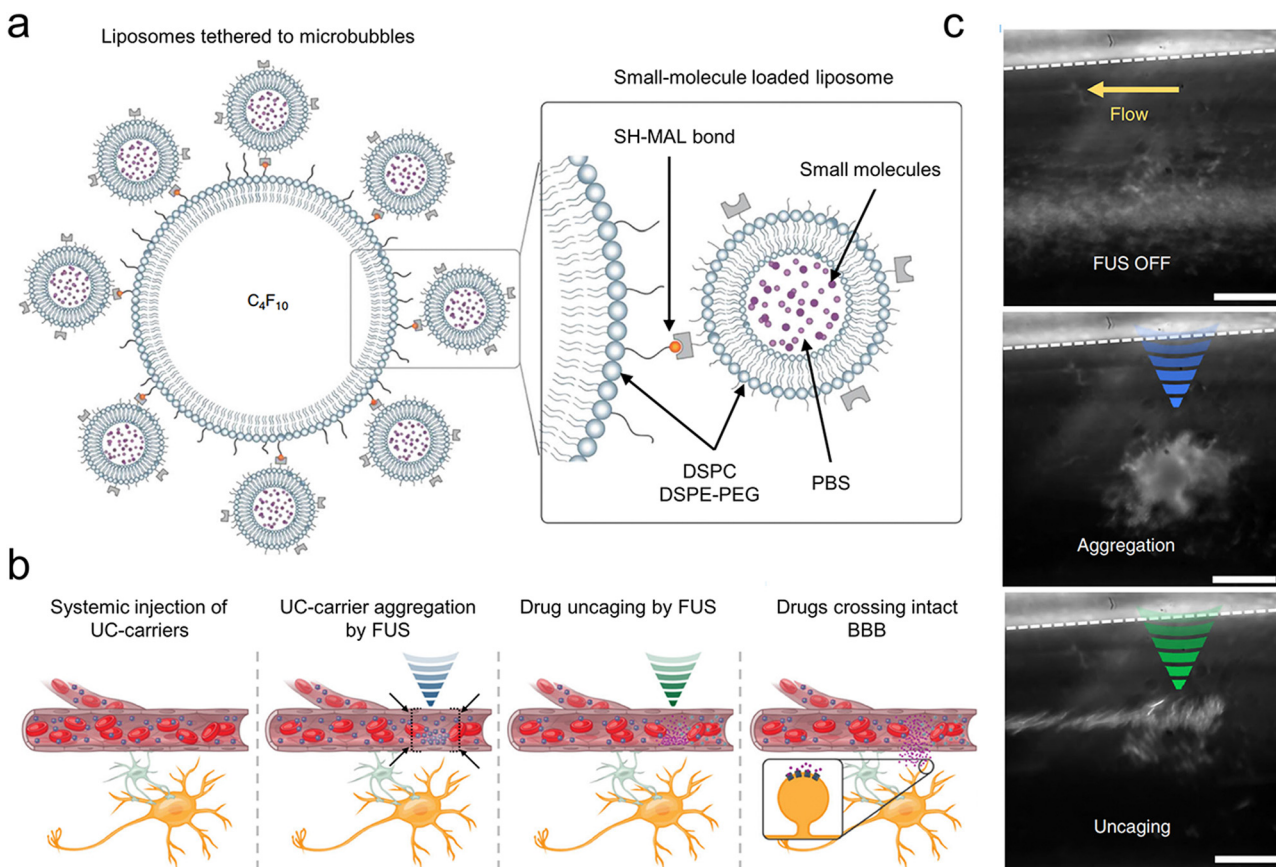


Fig. 9 (a) The design of a small-molecule-loaded carrier controlled by ultrasound (UC-carrier) made up of DSPC and DSPE-PEG2k. These materials form the outer layers of the microbubbles (single layer) and liposomes (double layer). (b) A diagram illustrating explains how these ultrasound-controlled drug carriers are gathered in one place and then opened to release their contents. (c) UC-carriers (seen as white spots in the picture) moving through a tube in microdialysis without the use of FUS (left), then clustering together (blue, middle) and finally being opened (green, right), which brings the UC-carriers together and lets out the small molecules. A dotted line indicates the tube's boundary. The scale bar is 50 μ m. Reproduced with permission.⁵⁴ Copyright 2020, Springer Nature.

drug—1300 times less than traditional systemic injection techniques—and requires significantly lower ultrasound pressure, 20 times beneath the FDA's diagnostic imaging safety limit. It enables molecularly specific, localized modulation with minimal side effects, paving new paths for treating brain diseases.

3.2.2. Sonodynamic mechanism. The sonodynamic mechanism mainly relies on sonosensitizers to produce ROS under US stimulation and is often used in the sonodynamic therapy of tumors.¹¹⁶ Rwei *et al.* introduce this technique for ultrasound-triggered local anesthesia.⁵⁸ US acted on the sonosensitizer protoporphyrin IX in liposomes to generate ROS, peroxidating unsaturated lipids in the bilayers and leading to the cargo release. *In vivo* experiments showed that the US-triggered release of tetrodotoxin from the liposomes could achieve repeatable nerve blocks in rats, and the duration of the effectiveness of the nerve block depended on the extent and intensity of the ultrasound waves used. No effective nerve block occurred below ultrasonic intensities of approximately 1 W cm^{-2} , above which the duration of the nerve block increased with ultrasound intensity. And insonation pulses of 2, 5 and 10 min induced nerve blocks with mean durations of 0.2 h, 0.5 h and 2.3 h, respectively. Thereby, adjustments of US parameters enable precise control over the release amount and duration of tetrodotoxin, facilitating accurate management of local anesthetic effects. Such control meets diverse pain management needs with high reproducibility and safety, offering safer and more personalized treatment options for patients.

Despite the promising prospects of US-triggered release for neuromodulation, several challenges, particularly concerning safety and drug delivery efficacy, remain to be addressed. The employment of perfluorocarbon-based systems, although therapeutically potential, involves a cavitation mechanism that incites safety concerns due to the risks associated with inertial cavitation and consequent microscale blood vessel deformations.¹¹⁷ Furthermore, the solubility of most drugs in perfluorocarbons is limited, curtailing the drug loading capacity within the particle shells. The ongoing refinement and exploration of these techniques not only promises to enrich our comprehension of neural circuits and signals but also to transform the treatment paradigm for neurological disorders.

3.3. Magnetic field-responsive

Magnetic fields, which do not necessitate direct contact with the patient's body and provide real-time magnetic response, are considered one of the most effective external physical stimuli for the precise activation of drug release. Techniques for magnetic field-based neuromodulation through controlled release rely on magnetic nanoparticles (MNPs) that can convert magnetic fields into signals recognized by biological receptors.^{118,119} These techniques are categorized into two principal types: magnetic-thermal mechanisms, which transform magnetic fields into heat, and magneto-mechanical mechanisms, which convert magnetic fields into force or torque. These mechanisms are discussed below.^{73,120}

3.3.1 Magnetic-thermal mechanism. Magnetic-thermal release of neuromodulators predominantly employs MNPs

and alternating magnetic fields (AMFs). The magnetism of MNPs is closely related to their size, morphology, and structure. For example, particles below the 50 nm threshold can achieve higher heating efficiency, related to the relaxation time of MNPs in AMF.¹²¹ When exposed to AMF with sufficient frequency and intensity, MNPs can transform AMF energy into heat *via* hysteresis loss, thereby eliciting biostimulation.¹²² Distinct from the photothermal mechanism, a small range of thermal induction *via* MNPs in AMFs triggers the local release of neuromodulatory compounds, thus circumventing the possibility of thermotoxicity in the whole brain region.

Introducing a change in the chemical structure of the delivery systems by the heat generated by MNPs is a strategy for magnetothermal triggered release. In a pivotal study, Romero *et al.* utilized 4,4'-azobis(4-cyanovaleric acid) (ACVA), a thermal labile linker, covalently bonded to iron oxide MNPs. The isothiocyanate (AITC), a TRPV1 calcium channel agonist, was then conjugated to ACVA.⁵⁹ ACVA was cleaved under the magnetothermal to release AITC, allowing calcium to flow in by activating TRPV1 channels and activating specific neurons. This approach achieved pharmacological excitation of ion channel function with a latency of around 12 s and low particle concentration (three orders of magnitude less) than the studies using bulk heating of magnetothermal effect. Park *et al.* devised a method for local pH adjustment by combining MNPs with polyanhydrides (or polyesters), whereby MNP-induced heating accelerates hydrolytic degradation of polymers.⁶⁰ This degradation releases carboxyl groups, leading to a localized pH reduction around the acid-sensing ion channel (ASIC) (Fig. 10(a)). The deployment of such chemomagnetic nanosensors to transform AMF signals into protons facilitates ASIC-mediated signaling in neurons (Fig. 10(b)) and modulates the activity of ASIC-abundant neurons in the brain (Fig. 10(c)), offering novel insights into proton-mediated ion channel activation within the nervous system.

Modulating the permeability of the liposome membrane through the heat generated by MNPs under AMFs is an alternative strategy for magnetothermal-triggered release. By elevating the external temperature beyond the phase transition temperature of the liposomes, their membrane shifts from a stable gel to a fluid state. This transition facilitates transient cavitation, characterized by microbubble formation and collapse, thereby enhancing membrane permeability.¹²³ For example, Rao *et al.* engineered temperature-sensitive nanoliposomes loaded with chemical payloads (drugs or receptor agonists and antagonists) and 25 nm iron oxide MNPs in the liposomes with a phase-transition temperature of 43 °C.⁶¹ *In vitro* release tests showed that the payload released due to local MNPs heating inside magnetic liposomes increased with the duration of AMF stimulation, while only a negligible increase in the temperature of the bulk solution was observed. This method allows for the precise and temporal modulation of specific neural activities by remotely controlling drug release at particular brain regions. Furthermore, the targeted delivery of chemomagnetic particles to the ventral tegmental area facilitates the remote modulation of motivated behavior in mice. Similarly, coating with thermosensitive polymers achieves comparable

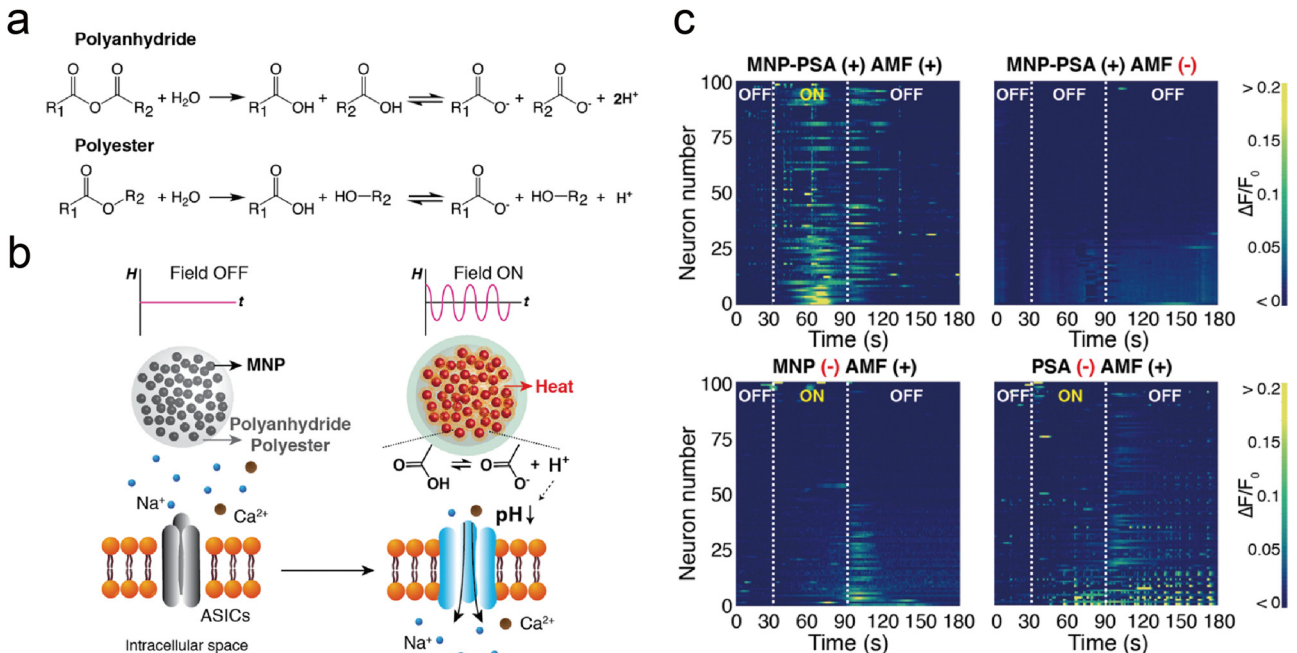


Fig. 10 (a) The hydrolytic breakdown processes of polyanhydride and polyester materials. (b) A visual depiction of a system capable of generating protons without the need for wired connections. (c) The presentation of individual fluo-4 fluorescence traces collected from 100 ASIC1a+ neurons, each subjected to varying experimental conditions. Reproduced with permission.⁶⁰ Copyright 2020, American Chemical Society.

outcomes. Guntnur *et al.* developed a method where MNPs were coated with thermoresponsive poly(oligo(ethylene glycol) methyl ether methacrylate) (POEGMA) brushes (Fig. 11(a)).⁶² These brushes collapsed upon heating, enabling the controlled release of dopamine through remote activation by AMF. This dopamine release amplified the response of dopamine ion channels on cell surfaces, boosting the activity of treated striatal neurons by approximately 50% (Fig. 11(b)). The applied 20 s of AMF was sufficient for MNPs to raise the local temperature and trigger the thermodynamic phase transition of POEGMA brush coating. During the 40 s of recovery, MNPs cooled down, allowing the reswelling of POEGMA brushes. The reversible thermodynamic phase transition of POEGMA brushes allowed for the on-demand release of dopamine in multiple microdoses to excite striatal neural activity (Fig. 11(c)). It is important to notice that this approach relies on local nanoscale heating effects. This method not only overcomes the possibility of therapeutic cargo degradation due to heat confinement inside the nano-carrier, but also offers reversible and safe temporal control over neuron-specific ligand–receptor interactions.

3.3.2 Magneto-mechanical mechanism. It is important to highlight that recent investigations have delved into the magneto-mechanical steering action of MNPs when subjected to a magnetic field. This mechanism facilitates remote manipulation of mechanical forces at the cellular or molecular scale at low-frequency AMFs without heat generation.^{124,125} In the study conducted by Kondaveeti *et al.*, magnetic-responsive hydrogels were formed by cross-linking alginate and xanthan gum with Ca^{2+} and *in situ* synthesis of MNPs.⁶³ The resultant repulsion or attraction between MNPs caused local compression and stretching of hydrogels under the external magnetic field and led to the levodopa release with a

release rate of $64 \pm 6\%$ of the initial load after 30 hours. The cell adhesion and proliferation of human neuroblastoma SH-SY5Y cells on the levodopa-loaded magnetic hydrogels were observed when exposed to the static external magnetic field. This study reveals a strategy for customizing and developing new biocompatible, magnetic-responsive materials for controlled levodopa release and the treatment of Parkinson's disease.

However, the caveat is that the translation of MNPs into clinical settings is hindered by challenges related to cytotoxicity, genotoxicity, *in vivo* metabolic pathways, and other safety concerns of MNPs, all of which require exhaustive evaluation. Consequently, the advancement of MNP-based drug delivery systems necessitates collaborative efforts across disciplines and detailed research to verify their safety and efficacy, as well as optimize their therapeutic potential.⁷³ Furthermore, achieving magnetochemical neuromodulation in cells and various neuron populations in larger animals, such as primates, remains an imperative goal.

4. Conclusions and perspective

In the evolving landscape of neurotherapeutics, stimuli-responsive controlled release systems stand at the forefront of innovation, offering promising avenues for precise, targeted, and minimally invasive neuromodulation. Recent advances in this field, propelled by nanotechnology, have brought us closer to addressing some persistent challenges in neuromodulation. Specifically, it has examined delivery systems that utilize various energy exchange modes to address the limitations associated with direct physical or chemical stimulation, such

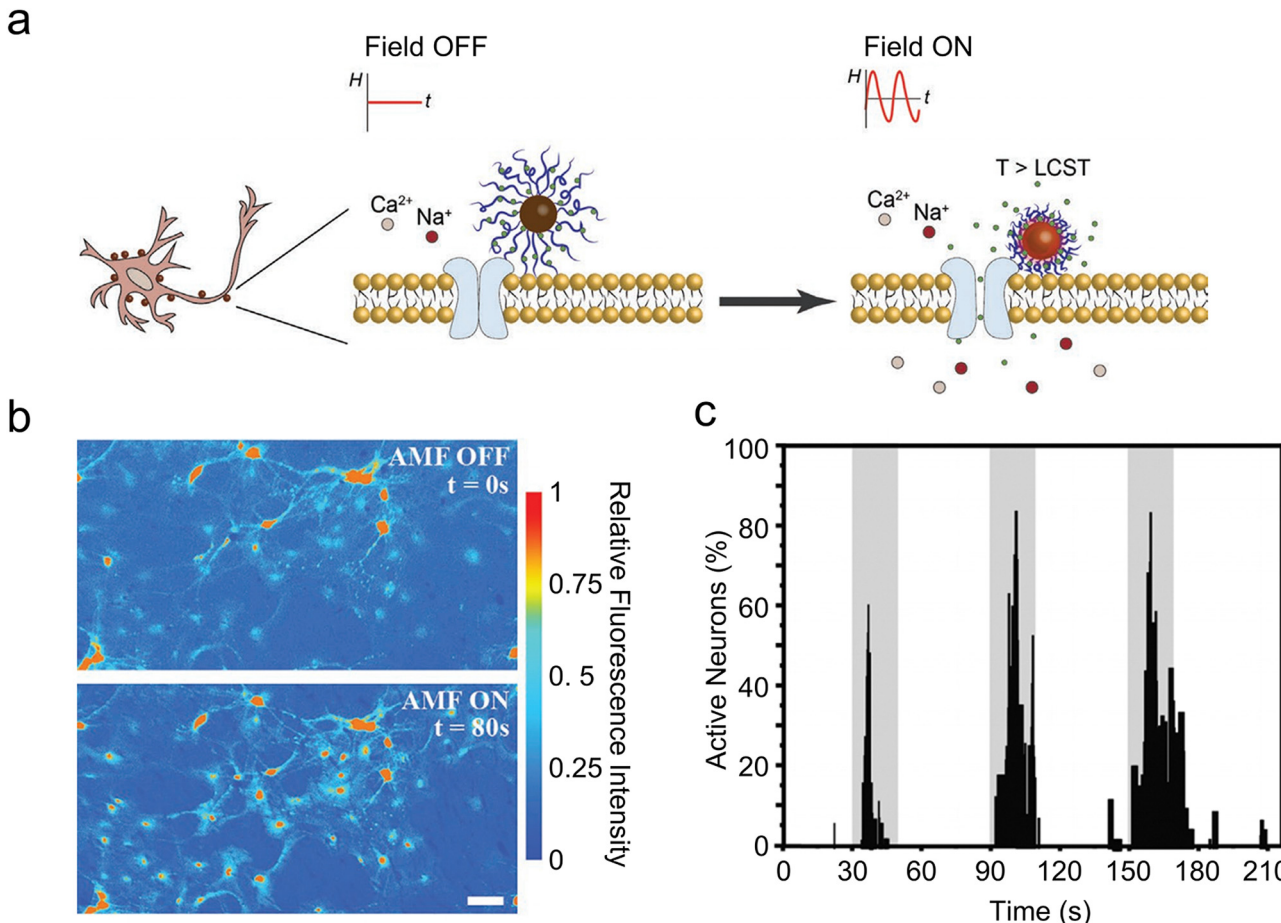


Fig. 11 (a) Chemomagnetic neuromodulation strategy of MNPs-POEGMA. (b) Calcium fluorescence images from a representative video of striatal neurons subjected to 1 min chemomagnetic stimulation by MNPs-POEGMA-DOP at the AMF conditions of 27.3 mT and 250 kHz. Scale bar = 30 μ m. (c) Normalized percentage of active neurons tracking the activity of 100 random striatal neurons co-cultured with MNPs-POEGMA-DOP and exposed to three cycles of AMF pulses of 20 s on–40 s off. AMF pulses are of 27.3 mT and 250 kHz. Reproduced with permission.⁶² Copyright 2022, Wiley-VCH.

as lack of specificity and invasiveness. However, there remains ample scope for improvement, especially from a material design standpoint.

First, enhancing the ability of these systems to penetrate the BBB with minimal invasiveness is crucial. The prevalent reliance on local injections presents a significant drawback, necessitating invasive procedures that heighten the risk of complications and restrict the broad applicability of these therapies. We should focus on exploring strategies for delivering these systems across the BBB into the central nervous system *via* transcellular or paracellular pathways, such as targeting receptors that promote endothelial transcytosis or transient opening BBB.¹²⁶ Designing materials and delivery systems capable of non-invasively overcome the BBB will not only expand the therapeutic window but also enhance patient compliance and curative effect. Second, it is vital to develop safer methods for neuromodulator release. While current techniques are effective, they can lead to undesirable side effects, such as heat generation or ROS production, negatively impacting neural activity and overall brain health. Innovating release mechanisms that avoid these complications, potentially

through the employment of biocompatible materials and energy-efficient stimuli (*e.g.*, the release triggered by nanomechanical force), is essential for reducing side effects and enhancing therapeutic efficacy. Thirdly, prioritizing the exploration of interactions between nanomaterials and the brain is indispensable. Despite significant progress in designing and applying nanomaterials for neuromodulation, investigations into their long-term effects on neural tissues and the brain's milieu are limited. Bridging this knowledge gap is imperative to confirm the safety, efficacy, and biocompatibility of these systems over prolonged durations. It necessitates to conduct thorough biocompatibility evaluations and detailed mechanistic analyses.

In conclusion, the latest developments in stimuli-responsive controlled release systems signal a new era in neuromodulation. Enhancing BBB penetration designs, formulating safer release techniques, and deepening our grasp of the nanomaterial-brain interface are essential research and development directions. Moreover, establishing clear, uniform criteria for toxicity and genotoxicity evaluation is crucial for the clinical development and application of these stimulus-responsive drug

delivery nanoplatforms. With ongoing technological innovation and interdisciplinary collaboration, the future is poised for realizing safer, more effective, and personalized neuroregulatory applications.

Author contributions

All authors conceptualized the article, wrote the original draft, and reviewed/edited the article. H. X. served as a project administrator and provided funding acquisition.

Conflicts of interest

There are no conflicts to declare.

Acknowledgements

This work was partially supported by the Science and Technology Program of Guangzhou (2024A04J4921 to H. X.), Guangdong Basic and Applied Basic Research Foundation (2023A1515110019 to H. X.), and Guangdong-Hong Kong Joint Laboratory for Psychiatric Disorders (2023B1212120004).

Notes and references

- 1 S. M. Won, E. Song, J. T. Reeder and J. A. Rogers, *Cell*, 2020, **181**, 115–135.
- 2 R. Chen, A. Canales and P. Anikeeva, *Nat. Rev. Mater.*, 2017, **2**, 16093.
- 3 D. C. Klooster, A. J. de Louw, A. P. Aldenkamp, R. M. Besseling, R. M. Mestrom, S. Carrette, S. Zinger, J. W. Bergmans, W. H. Mess, K. Vonck, E. Carrette, L. E. Breuer, A. Bernas, A. G. Tijhuis and P. Boon, *Neurosci. Biobehav. Rev.*, 2016, **65**, 113–141.
- 4 N. Samuel, M. Y. R. Ding, C. Sarica, G. Darmani, I. E. Harmsen, T. Grippe, X. Chen, A. Yang, N. Nasrkhani, K. Zeng, R. Chen and A. M. Lozano, *Mov. Disord.*, 2023, **38**, 2209–2216.
- 5 V. Jogpal, M. Sanduja, R. Dutt, V. Garg and Tinku, *Inflammopharmacology*, 2022, **30**, 355–368.
- 6 N. Vogt, *Nat. Methods*, 2019, **16**, 954.
- 7 S. M. Sternson and B. L. Roth, *Annu. Rev. Neurosci.*, 2014, **37**, 387–407.
- 8 M. R. Picciotto, M. J. Higley and Y. S. Mineur, *Neuron*, 2012, **76**, 116–129.
- 9 L. Speranza, U. di Porzio, D. Viggiano, A. de Donato and F. Volpicelli, *Cells*, 2021, **10**, 735.
- 10 Y. Wang, R. Garg, D. Cohen-Karni and T. Cohen-Karni, *Nat. Rev. Bioeng.*, 2023, **1**, 193–207.
- 11 Q. Jiang and S. Zhang, *Small*, 2023, **19**, 2206929.
- 12 M. Roet, S. A. Hescham, A. Jahanshahi, B. P. F. Rutten, P. O. Anikeeva and Y. Temel, *Prog. Neurobiol.*, 2019, **177**, 1–14.
- 13 H. Xiong, B. A. Wilson, P. A. Slesinger and Z. Qin, *ACS Chem. Neurosci.*, 2023, **14**, 516–523.
- 14 H. Xiong, E. Lacin, H. Ouyang, A. Naik, X. Xu, C. Xie, J. Youn, B. A. Wilson, K. Kumar, T. Kern, E. Aisenberg, D. Kircher, X. Li, J. A. Zasadzinski, C. Mateo, D. Kleinfeld, S. Hrabetova, P. A. Slesinger and Z. Qin, *Angew. Chem., Int. Ed.*, 2022, **61**, e202206122.
- 15 H. Lea-Banks, M. A. O'Reilly, C. Hamani and K. Hynnen, *Theranostics*, 2020, **10**, 2849–2858.
- 16 J. Wang, Q. Ni, Y. Wang, Y. Zhang, H. He, D. Gao, X. Ma and X.-J. Liang, *J. Controlled Release*, 2021, **331**, 282–295.
- 17 E. Blanco, H. Shen and M. Ferrari, *Nat. Biotechnol.*, 2015, **33**, 941–951.
- 18 M. Xu, Y. Qi, G. Liu, Y. Song, X. Jiang and B. Du, *ACS Nano*, 2023, **17**, 20825–20849.
- 19 N. J. Abbott, L. Rönnbäck and E. Hansson, *Nat. Rev. Neurosci.*, 2006, **7**, 41–53.
- 20 R. Pandit, L. Chen and J. Götz, *Adv. Drug Delivery Rev.*, 2020, **165–166**, 1–14.
- 21 X. Li, V. Vemireddy, Q. Cai, H. Xiong, P. Kang, X. Li, M. Giannotta, H. N. Hayenga, E. Pan, S. R. Sirsi, C. Mateo, D. Kleinfeld, C. Greene, M. Campbell, E. Dejana, R. Bachoo and Z. Qin, *Nano Lett.*, 2021, **21**, 9805–9815.
- 22 B. Oller-Salvia, M. Sánchez-Navarro, E. Giralt and M. Teixidó, *Chem. Soc. Rev.*, 2016, **45**, 4690–4707.
- 23 J. Xie, Z. Shen, Y. Anraku, K. Kataoka and X. Chen, *Biomaterials*, 2019, **224**, 119491.
- 24 S. Ding, A. I. Khan, X. Cai, Y. Song, Z. Lyu, D. Du, P. Dutta and Y. Lin, *Mater. Today*, 2020, **37**, 112–125.
- 25 G. C. Terstappen, A. H. Meyer, R. D. Bell and W. Zhang, *Nat. Rev. Drug Discovery*, 2021, **20**, 362–383.
- 26 M. Olsman, V. Sereti, M. Mühlenpfordt, K. B. Johnsen, T. L. Andresen, A. J. Urquhart and C. de L Davies, *Ultrasound Med. Biol.*, 2021, **47**, 1343–1355.
- 27 J. Wang, Z. Li, M. Pan, M. Fiaz, Y. Hao, Y. Yan, L. Sun and F. Yan, *Adv. Drug Delivery Rev.*, 2022, **190**, 114539.
- 28 H. Lea-Banks, Y. Meng, S.-K. Wu, R. Belhadjhamida, C. Hamani and K. Hynnen, *J. Controlled Release*, 2021, **332**, 30–39.
- 29 Z. Gao, E. T. David, T. W. Leong, X. Li, Q. Cai, J. Mwirigi, M. Giannotta, E. Dejana, J. Wiggins, S. Krishnagiri, R. M. Bachoo, T. J. Price and Z. Qin, *bioRxiv*, 2022, DOI: [10.1101/2022.05.20.492752](https://doi.org/10.1101/2022.05.20.492752).
- 30 R. G. Thorne and C. Nicholson, *Proc. Natl. Acad. Sci. U. S. A.*, 2006, **103**, 5567–5572.
- 31 J. Zámceník, L. Vargová, A. Homola, R. Kodet and E. Syková, *Neuropathol. Appl. Neurobiol.*, 2004, **30**, 338–350.
- 32 H. Xiong, E. Lacin, H. Ouyang, A. Naik, X. Xu, C. Xie, J. Youn, B. A. Wilson, K. Kumar, T. Kern, E. Aisenberg, D. Kircher, X. Li, J. A. Zasadzinski, C. Mateo, D. Kleinfeld, S. Hrabetova, P. A. Slesinger and Z. Qin, *Angew. Chem., Int. Ed.*, 2022, **61**, e202206122.
- 33 E. A. Nance, G. F. Woodworth, K. A. Sailor, T.-Y. Shih, Q. Xu, G. Swaminathan, D. Xiang, C. Eberhart and J. Hanes, *Sci. Transl. Med.*, 2012, **4**, 149ra119.
- 34 E. Song, A. Gaudin, A. R. King, Y.-E. Seo, H.-W. Suh, Y. Deng, J. Cui, G. T. Tietjen, A. Huttner and W. M. Saltzman, *Nat. Commun.*, 2017, **8**, 15322.
- 35 S. Dante, A. Petrelli, E. M. Petrini, R. Marotta, A. Maccione, A. Alabastri, A. Quarta, F. De Donato, T. Ravasenga,

A. Sathya, R. Cingolani, R. Proietti Zaccaria, L. Berdondini, A. Barberis and T. Pellegrino, *ACS Nano*, 2017, **11**, 6630–6640.

36 M. R. Banghart and B. L. Sabatini, *Neuron*, 2012, **73**, 249–259.

37 A. E. Layden, X. Ma, C. A. Johnson, X. J. He, S. A. Buczynski and M. R. Banghart, *J. Am. Chem. Soc.*, 2023, **145**, 19611–19621.

38 X. Ma, D. A. Johnson, X. J. He, A. E. Layden, S. P. McClain, J. C. Yung, A. Rizzo, J. Bonaventura and M. R. Banghart, *Nat. Methods*, 2023, **20**, 682–685.

39 S. P. McClain, X. Ma, D. A. Johnson, C. A. Johnson, A. E. Layden, J. C. Yung, S. T. Lubejko, G. Livrizzi, X. J. He, J. Zhou, J. Chang-Weinberg, E. Ventriglia, A. Rizzo, M. Levinstein, J. L. Gomez, J. Bonaventura, M. Michaelides and M. R. Banghart, *Neuron*, 2023, **111**, 3926–3940.

40 R. E. Kohman, S. S. Cha, H. Y. Man and X. Han, *Nano Lett.*, 2016, **16**, 2781–2785.

41 A. T. Veetil, K. Chakraborty, K. Xiao, M. R. Minter, S. S. Sisodia and Y. Krishnan, *Nat. Nanotechnol.*, 2017, **12**, 1183–1189.

42 Y. Jiang, P. Fu, Y. Liu, C. Wang, P. Zhao, X. Chu, X. Jiang, W. Yang, Y. Wu, Y. Wang, G. Xu, J. Hu and W. Bu, *Sci. Adv.*, 2020, **6**, eabc3513.

43 H. J. Xiong, K. A. Alberto, J. Youn, J. Taura, J. Morstein, X. Y. Li, Y. Wang, D. Trauner, P. A. Slesinger, S. O. Nielsen and Z. P. Qin, *Nano Res.*, 2023, **16**, 1033–1041.

44 A. Y. Rwei, B. Y. Wang, T. Ji, C. Zhan and D. S. Kohane, *Nano Lett.*, 2017, **17**, 7138–7145.

45 C. Zhan, W. Wang, J. B. McAlvin, S. Guo, B. P. Timko, C. Santamaria and D. S. Kohane, *Nano Lett.*, 2016, **16**, 177–181.

46 C. Zhan, W. Wang, C. Santamaria, B. Wang, A. Rwei, B. P. Timko and D. S. Kohane, *Nano Lett.*, 2017, **17**, 660–665.

47 B. Li, Y. Wang, D. Gao, S. Ren, L. Li, N. Li, H. An, T. Zhu, Y. Yang, H. Zhang and C. Xing, *Adv. Funct. Mater.*, 2021, **31**, 2010757.

48 W. Li, R. Luo, X. Lin, A. D. Jadhav, Z. Zhang, L. Yan, C. Y. Chan, X. Chen, J. He, C. H. Chen and P. Shi, *Biomaterials*, 2015, **65**, 76–85.

49 T. Nakano, S. M. Mackay, E. Wui Tan, K. M. Dani and J. Wickens, *eNeuro*, 2016, **3**, 6.

50 X. Li, Z. Che, K. Mazhar, T. J. Price and Z. Qin, *Adv. Funct. Mater.*, 2017, **27**, 1605778.

51 H. Xiong, X. Li, P. Kang, J. Perish, F. Neuhaus, J. E. Ploski, S. Kroener, M. O. Ogunyankin, J. E. Shin, J. A. Zasadzinski, H. Wang, P. A. Slesinger, A. Zumbuehl and Z. Qin, *Angew. Chem., Int. Ed.*, 2020, **59**, 8608–8615.

52 A. Y. Rwei, C. Zhan, B. Wang and D. S. Kohane, *J. Controlled Release*, 2017, **251**, 68–74.

53 A. Y. Rwei, J. J. Lee, C. Y. Zhan, Q. Liu, M. T. Ok, S. A. Shankarappa, R. Langer and D. S. Kohane, *Proc. Natl. Acad. Sci. U. S. A.*, 2015, **112**, 15719–15724.

54 M. S. Ozdas, A. S. Shah, P. M. Johnson, N. Patel, M. Marks, T. B. Yasar, U. Stalder, L. Bigler, W. von der Behrens, S. R. Sirsi and M. F. Yanik, *Nat. Commun.*, 2020, **11**, 4929.

55 R. D. Airan, R. A. Meyer, N. P. K. Ellens, K. R. Rhodes, K. Farahani, M. G. Pomper, S. D. Kadam and J. J. Green, *Nano Lett.*, 2017, **17**, 652–659.

56 J. B. Wang, M. Aryal, Q. Zhong, D. B. Vyas and R. D. Airan, *Neuron*, 2018, **100**, 728–738.

57 K. Cullion, A. Y. Rwei and D. S. Kohane, *Ther. Delivery*, 2018, **9**, 5–8.

58 A. Y. Rwei, J. L. Paris, B. Wang, W. Wang, C. D. Axon, M. Vallet-Regí, R. Langer and D. S. Kohane, *Nat. Biomed. Eng.*, 2017, **1**, 644–653.

59 G. Romero, M. G. Christiansen, L. Stocche Barbosa, F. Garcia and P. Anikeeva, *Adv. Funct. Mater.*, 2016, **26**, 6471–6478.

60 J. Park, A. Tabet, J. Moon, P. H. Chiang, F. Koehler, A. Sahasrabudhe and P. Anikeeva, *Nano Lett.*, 2020, **20**, 6535–6541.

61 S. Rao, R. Chen, A. A. LaRocca, M. G. Christiansen, A. W. Senko, C. H. Shi, P. H. Chiang, G. Varnavides, J. Xue, Y. Zhou, S. Park, R. Ding, J. Moon, G. Feng and P. Anikeeva, *Nat. Nanotechnol.*, 2019, **14**, 967–973.

62 R. T. Guntur, N. Muzzio, A. Gomez, S. Macias, A. Galindo, A. Ponce and G. Romero, *Adv. Funct. Mater.*, 2022, **32**, 2204732.

63 S. Kondaveeti, A. T. S. Semeano, D. R. Cornejo, H. Ulrich and D. F. S. Petri, *Colloids Surf., B*, 2018, **167**, 415–424.

64 Y. Lei, Y. Hamada, J. Li, L. Cong, N. Wang, Y. Li, W. Zheng and X. Jiang, *J. Controlled Release*, 2016, **232**, 131–142.

65 Y. Zuo, J. Ye, W. Cai, B. Guo, X. Chen, L. Lin, S. Jin, H. Zheng, A. Fang, X. Qian, Z. Abdelrahman, Z. Wang, Z. Zhang, Z. Chen, B. Yu, X. Gu and X. Wang, *Nat. Nanotechnol.*, 2023, **18**, 1230–1240.

66 Z. Liu, Q. Liu, B. Zhang, Q. Liu, L. Fang and S. Gou, *J. Med. Chem.*, 2021, **64**, 13853–13872.

67 J. Sun, W. Wang, X. Hu, X. Zhang, C. Zhu, J. Hu and R. Ma, *J. Nanobiotechnol.*, 2023, **21**, 58.

68 B. Pomierny, W. Krzyżanowska, J. Jurczyk, A. Skórkowska, B. Strach, M. Szafarz, K. Przejczońska-Pomierny, R. Torregrossa, M. Whiteman, M. Marcinkowska, J. Pera and B. Budziszewska, *Int. J. Mol. Sci.*, 2021, **22**, 7816.

69 H. A. Pal, S. Mohapatra, V. Gupta, S. Ghosh and S. Verma, *Chem. Sci.*, 2017, **8**, 6171–6175.

70 N. Fomina, J. Sankaranarayanan and A. Almutairi, *Adv. Drug Delivery*, 2012, **64**, 1005–1020.

71 R. Henry, M. Deckert, V. Guruviah and B. Schmidt, *IETE Tech. Rev.*, 2015, **33**, 368–377.

72 J. Blackmore, S. Shrivastava, J. Sallet, C. R. Butler and R. O. Cleveland, *Ultrasound Med. Biol.*, 2019, **45**, 1509–1536.

73 G. Romero, J. Park, F. Koehler, A. Pralle and P. Anikeeva, *Nat. Rev. Methods Primers*, 2022, **2**, 92.

74 S. Chen, A. Z. Weitemier, X. Zeng, L. M. He, X. Y. Wang, Y. Q. Tao, A. J. Y. Huang, Y. Hashimoto-dani, M. Kano, H. Iwasaki, L. K. Parajuli, S. Okabe, D. B. L. Teh, A. H. Ali, I. Tsutsui-Kimura, K. F. Tanaka, X. G. Liu and T. J. McHugh, *Science*, 2018, **359**, 679–683.

75 X. Wu, Y. Y. Jiang, N. J. Rommelfanger, F. Yang, Q. Zhou, R. K. Yin, J. L. Liu, S. Cai, W. Ren, A. Shin, K. S. Ong,

K. Y. Pu and G. S. Hong, *Nat. Biomed. Eng.*, 2022, **6**, 754–770.

76 G. Hong, A. L. Antaris and H. Dai, *Nat. Biomed. Eng.*, 2017, **1**, 0010.

77 X. Wu, F. Yang, S. Cai, K. Pu and G. Hong, *ACS Nano*, 2023, **17**, 7941–7952.

78 R. Weinstain, T. Slanina, D. Kand and P. Klán, *Chem. Rev.*, 2020, **120**, 13135–13272.

79 G. C. Ellis-Davies, *Nat. Methods*, 2007, **4**, 619–628.

80 H.-M. Lee, D. R. Larson and D. S. Lawrence, *ACS Chem. Biol.*, 2009, **4**, 409–427.

81 G. C. R. Ellis-Davies, *Acc. Chem. Res.*, 2020, **53**, 1593–1604.

82 M. R. Banghart and B. L. Sabatini, *Neuron*, 2012, **73**, 249–259.

83 B. Yang, T. T. Wang, Y. S. Yang, H. L. Zhu and J. H. Li, *J. Drug Delivery Sci. Technol.*, 2021, **66**, 102880.

84 T. Wang, Y. Liu, Q. Wu, B. Lou and Z. Liu, *Smart Mater. Med.*, 2022, **3**, 66–84.

85 D. Miao, Y. Yu, Y. Chen, Y. Liu and G. Su, *Mol. Pharmaceutics*, 2020, **17**, 1127–1138.

86 H. M. Bandara and S. C. Burdette, *Chem. Soc. Rev.*, 2012, **41**, 1809–1825.

87 D. Miranda and J. F. Lovell, *Bioeng. Transl. Med.*, 2016, **1**, 267–276.

88 T. K. Mukhopadhyay, J. Morstein and D. Trauner, *Curr. Opin. Pharmacol.*, 2022, **63**, 102202.

89 S. Kellner and S. Berlin, *Appl. Sci.*, 2020, **10**, 805.

90 C. Pernpeintner, J. A. Frank, P. Urban, C. R. Roeske, S. D. Pritzl, D. Trauner and T. Lohmüller, *Langmuir*, 2017, **33**, 4083–4089.

91 S. D. Pritzl, D. B. Konrad, M. F. Ober, A. F. Richter, J. A. Frank, B. Nickel, D. Trauner and T. Lohmüller, *Langmuir*, 2021, **38**, 385–393.

92 S. D. Pritzl, P. Urban, A. Prasselsperger, D. B. Konrad, J. A. Frank, D. Trauner and T. Lohmüller, *Langmuir*, 2020, **36**, 13509–13515.

93 P. Urban, S. D. Pritzl, D. B. Konrad, J. A. Frank, C. Pernpeintner, C. R. Roeske, D. Trauner and T. Lohmüller, *Langmuir*, 2018, **34**, 13368–13374.

94 P. Urban, S. D. Pritzl, M. F. Ober, C. F. Dirscherl, C. Pernpeintner, D. B. Konrad, J. A. Frank, D. Trauner, B. Nickel and T. Lohmüller, *Langmuir*, 2020, **36**, 2629–2634.

95 M. L. DiFrancesco, F. Lodola, E. Colombo, L. Maragliano, M. Bramini, G. M. Paternò, P. Baldelli, M. D. Serra, L. Lunelli, M. Marchioretto, G. Grasselli, S. Cimò, L. Colella, D. Fazzi, F. Ortica, V. Vurro, C. G. Eleftheriou, D. Shmal, J. F. Maya-Vetencourt, C. Bertarelli, G. Lanzani and F. Benfenati, *Nat. Nanotechnol.*, 2020, **15**, 296–306.

96 D. Liu, S. Wang, S. Xu and H. Liu, *Langmuir*, 2017, **33**, 1004–1012.

97 A. Torchì, F. Simonelli, R. Ferrando and G. Rossi, *ACS Nano*, 2017, **11**, 12553–12561.

98 D. Miranda and J. F. Lovell, *Bioeng. Transl. Med.*, 2016, **1**, 267–276.

99 K.-H. Shen, C.-H. Lu, C.-Y. Kuo, B.-Y. Li and Y.-C. Yeh, *J. Mater. Chem. B*, 2021, **9**, 7100–7116.

100 T. Hoare, S. Young, M. W. Lawlor and D. S. Kohane, *Acta Biomater.*, 2012, **8**, 3596–3605.

101 Y. Hou, X. Meng, S. Zhang, F. Sun and W. Liu, *Int. J. Pharm.*, 2022, **611**, 121315.

102 G. Wu, A. Mikhailovsky, H. A. Khant, C. Fu, W. Chiu and J. A. Zasadzinski, *J. Am. Chem. Soc.*, 2008, **130**, 8175–8177.

103 X. Li, P. Kang, Z. Chen, S. Lal, L. Zhang, J. J. Gassensmith and Z. Qin, *Chem. Commun.*, 2018, **54**, 2479–2482.

104 J. E. Shin, M. O. Ogunyankin and J. A. Zasadzinski, *Sci. Rep.*, 2020, **10**, 1706.

105 S. Jones, D. Andrén, T. J. Antosiewicz and M. Käll, *Nano Lett.*, 2019, **19**, 8294–8302.

106 Y. Huang, P. Huang and J. Lin, *Small Methods*, 2019, **3**, 1800394.

107 J. Randrianalisoa, X. Li, M. Serre and Z. Qin, *Adv. Opt. Mater.*, 2017, **5**, 1700403.

108 F. Neuhaus, D. Mueller, R. Tanasescu, S. Balog, T. Ishikawa, G. Brezesinski and A. Zumbuehl, *Langmuir*, 2018, **34**, 3215–3220.

109 F. Neuhaus, D. Mueller, R. Tanasescu, S. Balog, T. Ishikawa, G. Brezesinski and A. Zumbuehl, *Angew. Chem., Int. Ed.*, 2017, **56**, 6515–6518.

110 Y. Xu, X. Dong, H. Xu, P. Jiao, L. X. Zhao and G. Su, *Pharmaceutics*, 2023, **15**, 2309.

111 S. Ibsen, A. Tong, C. Schutt, S. Esener and S. H. Chalasani, *Nat. Commun.*, 2015, **6**, 8264.

112 Y. Song, T. Hahn, I. P. Thompson, T. J. Mason, G. M. Preston, G. Li, L. Paniwnyk and W. E. Huang, *Nucleic Acids Res.*, 2007, **35**, e129.

113 A. Dasgupta, M. Liu, T. Ojha, G. Storm, F. Kiessling and T. Lammers, *Drug Discovery Today: Technol.*, 2016, **20**, 41–48.

114 R. Airan, *Science*, 2017, **357**(6350), 465.

115 H. Lea-Banks, M. A. O'Reilly and K. Hynynen, *J. Controlled Release*, 2019, **293**, 144–154.

116 D. Costley, C. Mc Ewan, C. Fowley, A. P. McHale, J. Atchison, N. Nomikou and J. F. Callan, *Int. J. Hyperthermia*, 2015, **31**, 107–117.

117 H. Chen, W. Kreider, A. A. Brayman, M. R. Bailey and T. J. Matula, *Phys. Rev. Lett.*, 2011, **106**, 034301.

118 H. Wei, Y. Hu, J. Wang, X. Gao, X. Qian and M. Tang, *Int. J. Nanomed.*, 2021, **16**, 6097–6113.

119 Y. Hu, D. Li, H. Wei, S. Zhou, W. Chen, X. Yan, J. Cai, X. Chen, B. Chen, M. Liao, R. Chai and M. Tang, *Int. J. Nanomed.*, 2021, **16**, 4515–4526.

120 A. Salvatore, C. Montis, D. Berti and P. Baglioni, *ACS Nano*, 2016, **10**, 7749–7760.

121 R. Munshi, S. M. Qadri, Q. Zhang, I. Castellanos Rubio, P. Del Pino and A. Pralle, *eLife*, 2017, **6**, e27069.

122 J. Carrey, B. Mehdaoui and M. Respaud, *J. Appl. Phys.*, 2011, **109**, 8.

123 K. Sou, D. L. Le and H. Sato, *Small*, 2019, **15**, 1900132.

124 J.-u Lee, W. Shin, Y. Lim, J. Kim, W. R. Kim, H. Kim, J.-H. Lee and J. Cheon, *Nat. Mater.*, 2021, **20**, 1029–1036.

125 S. Jeong, W. Shin, M. Park, J.-u Lee, Y. Lim, K. Noh, J.-H. Lee, Y.-W. Jun, M. Kwak and J. Cheon, *Nano Lett.*, 2023, **23**, 5227–5235.

126 D. Furtado, M. Björnalm, S. Ayton, A. I. Bush, K. Kempe and F. Caruso, *Adv. Mater.*, 2018, **30**, e1801362.